Astron. Astrophys. 113, 61–72 (1982)

ASTRONOMY AND ASTROPHYSICS

Study of Spiral Galaxies from 392 New Measurements of 21-cm Line Data

L. Bottinelli[1], L. Gouguenheim[1], and G. Paturel[2]

[1] Observatoire de Meudon, Département de Radioastronomie, F-92190 Meudon, France et Université de Paris-Sud, Centre d'Orsay, F-91405 Orsay Cedex, France
[2] Observatoire de Lyon, F-69230 Saint Genis-Laval, France

Received March 25, 1981; accepted April 30, 1982

Summary. 392 spiral galaxies with type Sb or later have been detected in the 21-cm line of neutral hydrogen with the Nançay radiotelescope, and among them 172 H I fluxes are obtained for the first time. The source of any possible bias has been carefully analyzed and only the Malmquist bias appears to be significant. In order to obviate this observational effect, the range of radial velocities has been properly truncated for all statistical studies.

A mean value of each global parameter has been determined for each morphological type and compared to previous results. The internal dispersion of individual values has been analyzed. It appears first that this dispersion can be reduced when better distances than those deduced from the Hubble ratio are used. The distance scale determined by de Vaucouleurs reduces significantly the dispersion observed for all the parameters. As a first step, since such distance moduli are not yet available for all the galaxies of our sample, the distances have been determined from the Hubble ratio taking into account the H_0 variations with supergalactic coordinates as described by de Vaucouleurs and Bollinger.

Part of the internal dispersion seems to be intrinsic. In particular it appears that isolated galaxies could have a larger H I content, as indicated by their larger M_H/L_0 ratio implying either a larger H I content or a lower luminosity.

The luminosity effect on this last ratio has been studied using the corrected line width ΔV_0 as an indicator of luminosity, in order to avoid regression effects. No significant effect is found in our unbiased sample, which confirms a result previously given by Shostak.

Key words: spiral galaxies – 21-cm line radiation – neutral hydrogen – interstellar matter

I. Introduction

This program of systematic observations of a large number of galaxies with the Nançay radiotelescope in the 21-cm line of neutral hydrogen has been undertaken some years ago. The 21-cm line profile provides data for determining the total mass and the neutral hydrogen mass of galaxies together with the systemic radial velocity.

Previous studies of integral properties of galaxies have shown some correlations between the various parameters related to a galaxy, such as morphological type, luminosity, total mass or H I mass (Gouguenheim, 1969; Roberts, 1969, 1976; Balkowski, 1973; Lewis and Davies, 1973; Shostak, 1978). For example, the ratios of the H I mass-to-total mass M_H/M_i, and of H I mass-to-luminosity M_H/L_0, both increase towards later types, indicating that the Hubble sequence could be ordered by the increasing importance of the relative gas content in a galaxy. However, these correlations show a large scatter: within a given type, the scatter can be comparable to the entire range of the ratio from early spirals to irregulars.

This scatter may result from uncertainties in the measured parameters including the optical and radio data and the distances. However, it appears to be larger than expected from the errors quoted on the various parameters involved and the possible existence of a second independent variable, such as luminosity, has been discussed. In particular a dependence of the M_H/L_0 ratio with the luminosity is expected from theoretical reasons (Strom, 1980) in agreement with previous statistical results (Balkowski, 1973; Bottinelli and Gouguenheim, 1974), but more recent works, dealing with a larger number of data have not confirmed this dependence (Shostak, 1978; Bottinelli et al., 1980a).

It appears clearly today that the present properties of a galaxy depend not only on the initial conditions prevailing at the time of the galaxy formation but also on the relations with the neighbourhood. For example, some recent studies have shown that galaxies members of clusters appear to be neutral hydrogen deficient (Huchtmeier et al., 1976; Sullivan and Johnson, 1978; Krumm and Salpeter, 1979; Chamaraux et al., 1980; Balkowski and Chamaraux, 1981). It has been also suggested that the presence of companions could enhance star formation (Madore, 1980).

It is the aim of the present paper to study these correlations and their scatter from a homogeneous set of a larger number of data. About 450 galaxies with type ranging from Sa to irregulars have been observed at Nançay. The results concerning the early type spirals have been published in separate papers (Bottinelli et al., 1980a, b). The present paper gives the results for later types, ranging from Sb to irregular.

The sample is discussed in Sect. II, the influence of the distances adopted is discussed in Sect. III, various possible bias are investigated in Sect. IV, the results are given in Sect. V and the dependence of M_H/L_0 on the galaxy neighbourhood and on the luminosity is discussed in Sect. VI.

II. Observations and Properties of the Sample

The observations have been carried out with the Nançay radiotelescope. The half-power beamwidth is 4′ (E – W) by 22′ (N – S), (for

Send offprint requests to: L. Bottinelli

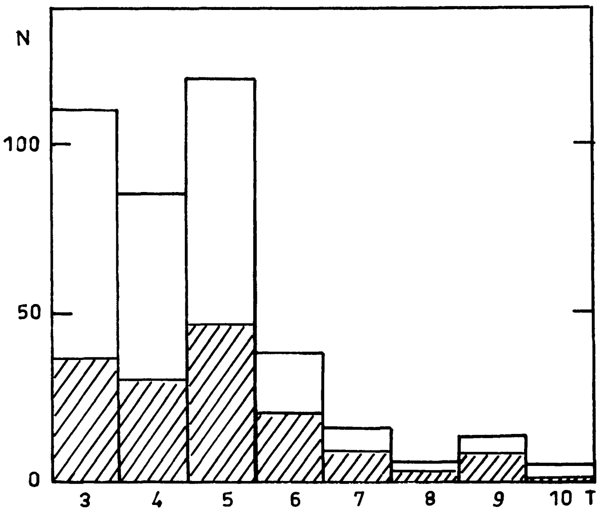

Fig. 1. Histogram of morphological types, coded according to the RC2, for the measured galaxies. The hatched region corresponds to our restricted sample

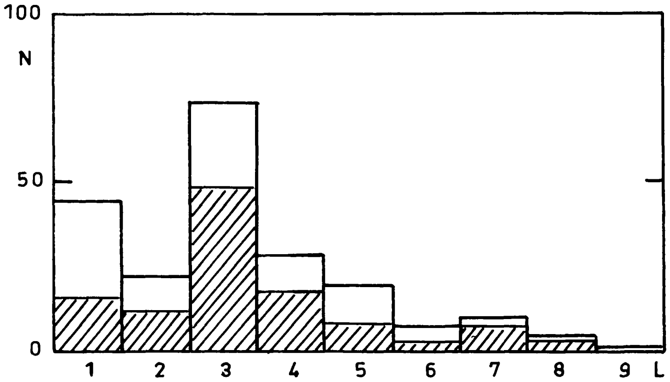

Fig. 2. Histogram of luminosity classes, coded according to the RC2, for the measured galaxies. The hatched region corresponds to our restricted sample

---

declination lower than 30°) at 21-cm wavelength. The total system temperature was 120 K and use was made of 15 channels spaced by 63.5 km s^{-1}, with a half power resolution of 63.5 km s^{-1}. The usual on and off procedure was used. Typical on-source integration time was ≈40 min. Use was made also in some cases of 32 channels spaced by 12.6 km s^{-1} with a half power resolution of 12.6 km s^{-1}. The galaxies have been observed at the positions given by Gallouët and Heidmann (1971) and Gallouët et al. (1973, 1975). When not given by these authors, the coordinates have been checked from the Palomar sky survey prints. All the galaxies with a photometric apparent E – W diameter (in the Holmberg system) larger than 3′ have been also observed at adjacent E – W positions (±4′ or ±8′ from the center). Due to the large N – S beam, possible confusion was checked from the PSS prints.

The integrated line profiles are published in a companion paper (Bottinelli et al., 1982b) with individual comments on galaxies. The following observational parameters have been deduced for each galaxy: (i) the *systematic radial velocity* as given in Bottinelli et al. (1981), (ii) the 21-cm *line width* ΔV measured at the 20 % level and corrected for bandwidth effect (Bottinelli et al., 1982a), (iii) the *total* H I *flux* obtained from the area under the total integrated line profile, following the method given by Gouguenheim (1969) through the formula:

$$F_{\rm H}(0) = 2.36\ 10^{-4}\ I_a C_F \ (\text{in } 10^6\ M_\odot\ \text{Mpc}^{-2}),$$

where I_a is the area under the line profile expressed in 10^{-3} flux unit km s^{-1} (lf.u. = 10^{-26} W m^{-2} Hz^{-1}) and C_F the 21-cm self-absorption correction which will be discussed in Sect. IV. H I fluxes are given here for the first time for 172 galaxies; these are noted in Table 2, Column 7. There are 71 galaxies in common with the sample of 169 late-type galaxies studied by Shostak (1978). A comparison of the H I fluxes $(F_{\rm H})_N$ and $(F_{\rm H})_S$ measured here and by Shostak respectively, gives the mean value of $(F_{\rm H})_N/(F_{\rm H})_S$ equal to 0.95 with a r.m.s. dispersion equal to 0.24, after rejecting NGC 1832, 1961, 2336, 5954, 6643, 6836, and 7137 which give somewhat discrepant results. The two flux scales appear thus to be in agreement within the errors.

For each galaxy the optical data have been obtained in the following way. All the morphological types are taken from the RC2 catalogue (de Vaucouleurs et al., 1976). The isophotal diameters a_{25} in arc min at the 25 mag arc s^{-2} brightness level are taken in the RC2 or when not available in the UGC catalogue (Nilson, 1973). In this last case the original UGC diameters are converted to the a_{25} diameters according to the relation given in the RC2. The axis ratio $\log R_{25} = \log(a_{25}/b_{25})$ are obtained in the same way.

The blue total magnitudes B_T are also taken in the RC2 where they result sometimes from the Harvard magnitudes converted to the B_T system. When not available in the RC2, they come from Zwicky CGCG magnitudes (Zwicky et al., 1961–1968) converted into B_T system according to the procedure explained in the appendix where it is shown that there is no systematic difference neither in the scale nor in the zero point between the B_T system and our reduced system.

Finally, the optical parameters B_T and $\log a_{25}$ are reduced to the galactic pole and zero inclination and redshift using the formulae given in the RC2, in the same way as in our previous paper (Bottinelli et al., 1980a). Thus the corrected parameters B_T^0 and a_{25}^0 are obtained.

The total sample contains 392 galaxies with morphological types Sb or later. The morphological types are coded according to the RC2. Their histogram, shown in Fig. 1, suggests to consider 5 classes:

Class 1: Type 3 (110 galaxies)
Class 2: Type 4 (85 galaxies)
Class 3: Type 5 (119 galaxies)
Class 4: Type 6 (38 galaxies)
Class 5: Type 7 and later (40 glaxies).

A special effort has been made to observe Sb galaxies and also galaxies with low declinations (down to −38°) which were not included in Shostak's sample.

The luminosity class index, taken from the RC2 is used to characterize the luminosity range covered by our sample (Fig. 2). It can be seen that all luminosity classes are represented, but the less luminous galaxies are somewhat deficient.

Another important characteristic of the sample is given by the histogram of the radial velocities (Fig. 3), in particular because the distance D will be calculated from the Hubble parameter H_0 using the relation: $D = V_0/H_0$, V_0 being the radial velocity with respect to the Local group of galaxies. The use of the Hubble relation as a distance indicator is suitable to our sample owing to the small number of low-velocity galaxies.

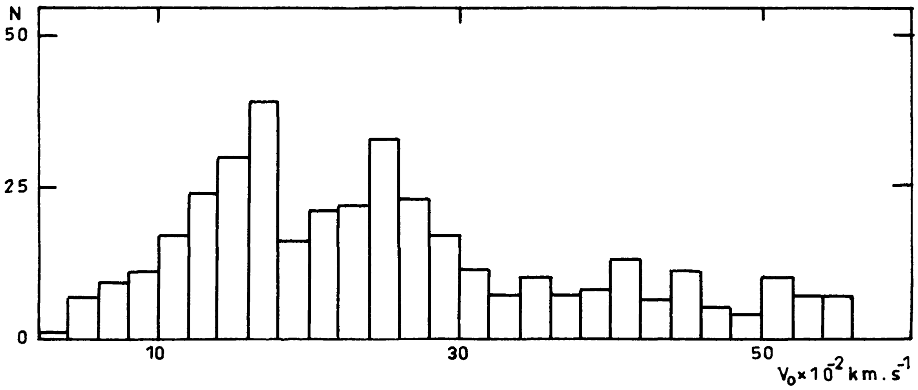

Fig. 3. Histogram of radial velocities V_0 with respect to the Local Group for the measured galaxies

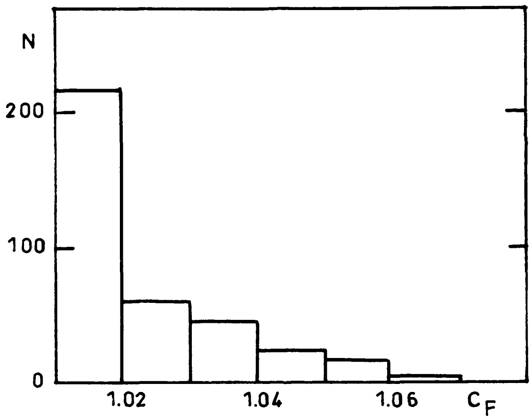

Fig. 4. Histogram of self-absorption correcting factors C_F for the measured galaxies: $C_F = F_H(0)/F_H(i)$ gives the corrected H I flux $F_H(0)$ from the observed H I flux $F_H(i)$ for a galaxy having an inclination i

The following integral parameters are deduced from the primary observational quantities: the linear diameter A_{25}^0, the intrinsic luminosity L_0, the corrected line width at the 20% level ΔV_0 corrected for inclination effect, the total hydrogen mass M_H, the mean neutral hydrogen projected density σ_H, the indicative total mass M_i and the mean indicative total mass projected density σ_i obtained from the following relations:

$A_{25}^0 = 0.2909\ D a_{25}^0$ (in kpc)
$L_0 = 1459\ D^2\ 10^{-0.4 B_T^0}$ (in $10^9\ L_\odot$ with $M_\odot = 5.41$)
$\Delta V_0 = \Delta V/\sin i$ (in km s^{-1})
$M_H = 10^{-3}\ F_H^0\ D^2$ (in $10^9\ M_\odot$)
$\sigma_H = 3.1\ F_H^0/(a_{25}^0)^2$ (in 10^{-3} g/cm^{-2})
$M_i = 3\ 10^{-5}\ A_{25}^0\ (\Delta V_0)^2$ (in $10^9\ M_\odot$)
$\sigma_i = 3.1\ 10^3\ M_i D^{-2}\ (a_{25}^0)^{-2}$ (in 10^{-3} g cm^{-2}),

where D is expressed in Mpc, a_{25}^0 in arc min, ΔV in km s^{-1}, F_H^0 in $10^6\ M_\odot$ Mpc^{-2}. The inclination i has been determined as explained by Bottinelli et al. (1980a).

The determination of some parameters depends on the distance. Our first problem is then to look for the best distance determinations.

Table 1. Dispersion of mean integral parameters for each morphological type

T (1)	(2)	μ (3)	H_0=100 (4)	H_0=100 (5)	H_0=H_0^* (6)
3	L_0	0.128(50)	0.348(50)	0.365(99)	0.364(99)
	A_{25}^0	0.101(51)	0.204(50)	0.217(109)	0.219(109)
	M_H	0.366(51)	0.412(49)	0.407(108)	0.402(107) [0.404]
	M_i	0.367(50)	0.450(49)	0.502(105)	0.454(103)
4	L_0	0.137(52)	0.289(54)	0.323(82)	0.310(82)
	A_{25}^0	0.098(54)	0.160(54)	0.193(85)	0.182(85)
	M_H	0.265(53)	0.321(53)	0.356(83)	0.321(83) [0.321]
	M_i	0.279(50)	0.355(50)	0.404(81)	0.388(81)
5	L_0	0.185(66)	0.366(66)	0.383(112)	0.378(112)
	A_{25}^0	0.093(66)	0.192(66)	0.196(119)	0.189(119)
	M_H	0.240(66)	0.325(66)	0.388(119)	0.366(119) [0.366]
	M_i	0.355(60)	0.450(60)	0.432(110)	0.411(109)
6	L_0	0.222(21)	0.316(21)	0.339(36)	0.333(36)
	A_{25}^0	0.095(21)	0.140(21)	0.191(38)	0.187(38)
	M_H	0.254(21)	0.358(21)	0.338(38)	0.320(38) [0.323]
	M_i	0.233(19)	0.304(19)	0.311(35)	0.301(35)
≥7	L_0	0.327(13)	0.370(13)	0.491(34)	0.464(34)
	A_{25}^0	0.195(13)	0.181(13)	0.241(40)	0.226(40)
	M_H	0.524(13)	0.587(13)	0.492(40)	0.472(40) [0.474]
	M_i	0.473(13)	0.522(13)	0.459(38)	0.453(38)

The logarithmic dispersions of integral parameters: L_0 (luminosity in $10^9\ L_\odot$), A_{25}^0 (linear diameter in kpc), M_H (hydrogen mass in $10^9\ M_\odot$), M_i (indicative total mass in $10^9\ M_\odot$) deduced from the number of data indicated in parentheses, are given (after 2σ rejection) when using the following distances to determine the mean value within a morphological type:
(i) Distance moduli μ from de Vaucouleurs (1979), in Column 3
(ii) V_0/H_0 with $H_0 = 100$ km s^{-1} Mpc^{-1}, in Columns 4 and 5
(iii) V_0/H_0^* with H_0^* given by de Vaucouleurs and Bollinger (1979).
Results to be compared are those in Columns 3 and 4 which refer to the same sample of galaxies having μ values on the one hand and those in Columns 5 and 6 which refer to the larger sample of galaxies having distances from a Hubble constant (see text) on the other hand. The dispersion from M_H values uncorrected for self-absorption is indicated between square brackets in Column 6

III. Discussion of the Distances

The distance moduli obtained by de Vaucouleurs (1979 and private communication) from optical data only are available for 205 galaxies belonging to our sample. In order to compare this distance scale and that deduced from a constant Hubble flow, assuming a value $H_0 = 100$ km s^{-1} Mpc^{-1} for the Hubble constant, the mean values of four parameters (luminosity, linear diameter, neutral

Table 2. Integral properties of measured galaxies

Name	T	i	L_o ($10^9 L_\odot$)	A^o_{25} (kpc)	D (Mpc)	M_H ($10^9 M_\odot$)	M_i ($10^9 M_\odot$)	σ_H (mg. cm^{-2})	σ_i (mg. cm^{-2})	M_H/L_o ($M_\odot/L_\odot$)	M_i/L_o ($M_\odot/L_\odot$)	M_H/M_i (×100)	
1	2	3	4	5	6	7	8	9	10	11	12	13	14
N 95	5	38	26.94	28.41	51.8	18.35*	357.4	5.96	116.1	68	13.27	5 13	
N 99	6	21	16.38	25.03	50.6	5 78*	127.0	2.42	53.1	.35	7.75	4.56	
N 100	6	86	.85	10.66	9.5	1.28	19.1	2.95	44.0	1.51	22.52	6 70	
N 131	3	76		6.33	12.8	1.70*	3.7	11 11	23.9			46.48	+
N 134	4	74	20.26	27.10	14.3	10.08	198.1	3.60	70.8	.50	9.78	5.09	+
N 145	8	38	15.18	20 18	39.0	4.44*	31.8	2.86	20.5	29	2 10	13.96	+
N 150	3	58	8.59	16.16	14 6	2 94*	62.1	2.95	62.3	.34	7.23	4.73	
N 151	4	61	32.78	34.16	35.4	6.28	312.1	1.41	70.2	.19	9.52	2.01	
N 157	4	48	18.55	18.93	16.0	4.72	90.4	3 46	66.2	.25	4.87	5.22	
N 173	4	25	8 50	43.38	41.1	9.18	830.0	1.28	115 7	1 08	97.69	1.11	
N 178	9	54	2.28	7.32	13.9	1.16*	2 5	5.67	12.1	.51	1.08	47 09	
N 180	4	34	13.56	37.49	48.9	4 50*	501 2	.84	93.6	33	36 95	.90	+
N 210	3	47	9.78	22.85	15.2	6.46	187.1	3 24	94.0	.66	19 14	3.45	
N 214	5	40	25.56	26.02	43.2	4 13*	225.9	1 60	87.5	16	8.84	1.83	
N 237	6	48	11 58	19.44	39.7	5 93*	170.4	4.11	118.3	.51	14.71	3.48	
N 255	4	27	4.96	13.95	15.3	1.88	76.4	2.53	102.9	38	15.41	2.46	
N 257	6	43	21.45	29 10	49.5	4.82*	261.0	1 49	80 8	.22	12 17	1.85	+
N 275	6	40	3 11	7.19	16.7	1.67	43 9	8 45	222 7	.53	14.11	3.79	
N 289	4	44	8.17	15.60	14.9	7.76	73.4	8 36	79 1	.95	8.99	10.58	
N 337	7	44	7.12	12.19	15.9	2 33	42.0	4.11	74.0	.33	5.90	5 55	
N 450	6	36	5.67	15.93	17.1	1 79	45.6	1.85	47 1	.31	8.03	3 92	
N 470	3	50	9.41	18.75	22.4	2 38	247 4	1.78	184.6	.25	26 30	96	+
N 488	3	40	32.35	33.12	22.0	3.00	1070.	72	255.8	.09	33.06	.28	
N 493	6	70	7.42	20.35	22.4	3.84*	55.9	2.43	35.4	52	7.54	6.87	
N 496	4	57	16.36	26.93	57.2	7.63*	164.1	2.76	59.4	.47	10.03	4 65	
N 514	5	34	11.63	24 21	24.0	4.03	172.9	1.80	77.4	35	14.87	2.33	
N 521	4	21	44.51	48.46	47.8	4.72	630.8	53	70.5	.11	14 17	.75	
N 578	5	49	12.40	20.37	15.4	3.91*	66.8	2.47	42.2	.32	5.39	5.86	
N 600	7	30	3.78	17.67	17.5	1.48*	7.9	1.24	6 6	.39	2.08	18.79	
N 613	4	38	16.79	22.11	13.4	2.02*	267.5	1 09	143.5	.12	15.93	.76	
N 615	3	66	8.21	17.48	17.5	1 81	106.6	1.55	91.6	.22	12.99	1.69	
N 658	3	57	9.55	24 75	28.6	5.89	190 3	2.52	81.5	.62	19.94	3.09	
N 673	5	38	30.38	33.76	48.8	7.26*	288.9	1.67	66.5	.24	9.51	2.51	
N 678	3	83	17.63	29.32	27 1	1 34	170.6	.41	52.1	.08	9.68	78	
N 691	4	40	6.69	26.11	26.0	3 42	469.5	1.32	180.6	51	70.18	.73	
N 697	4	70	21.33	34.40	30.0	13.48	264 6	2.99	58.6	63	12.40	5.10	
N 701	5	60	4.44	11.22	17.2	1.82	43 9	3.79	91.3	.41	9.88	4.15	+
N 706	3	40	30.80	30.14	46.6	3.17*	161.3	.92	46.6	.10	5.24	1.97	+
N 753	4	43	32.67	39.14	46.4	8.09	354.9	1.39	60.8	.25	10.86	2 28	
N 755	3	71		14.82	15.3	2.12*	36.8	2.53	43.9			5.77	
N 772	3	52	43.83	46.33	23.6	10.31	418 6	1.26	51.2	.24	9.55	2 46	+
N 779	3	73	7.41	12.61	13.0	1.58	81.5	2.60	134.4	.21	11.00	1 93	
N 864	5	40	10.75	19.70	15.0	3.75	91.6	2.53	61.9	35	8.51	4.10	
N 871	5	67	6.43	11.55	35.1	4.71	27.2	9.26	53.5	73	4.22	17.32	
N 876	5	78	1.57	16.96	36.4	12.30	84.2	11.21	76.8	7.81	53.49	14.60	+
N 877	4	40	28.40	25.11	36.9	8.68	336.7	3.61	140.0	.31	11.86	2.58	+
N 895	6	41	11.53	22.07	21.3	5.02	130.3	2.71	70.2	.44	11.30	3.86	
N 907	7	70		7 23	15.6	.60*	8.7	3.02	43.4			6.97	
N 908	5	61	17.99	19 08	13.4	1.43*	138.1	1.03	99.6	.08	7.68	1.04	
N 922	6	24	14.13	16 09	27.9	5 07	127 2	5 14	129 0	.36	9.00	3 99	+
N 958	5	69	44.52	35.88	53.1	21.08*	141.9	4.29	28 9	.47	3.19	14.86	
N 991	5	21	4 17	11 48	14 1	79*	12.5	1 56	24.9	.19	2.99	6.30	
N1003	6	68	2.62	10.18	7 4	1.17	20.1	2.97	50.9	.45	7.68	5.83	
N1058	5	17	1 36	5 81	6.1	84		6.54		.62			
N1073	5	21	6 34	16 86	11.4	2 38*	21.7	2.19	20.0	.37	3.42	10.95	
N1084	5	59	11.68	9 84	12.9	2 39	45.1	6.46	122 0	.20	3.86	5.30	
N1087	5	48	10.22	13.70	14.1	1.55	39.7	2.17	55.4	15	3.88	3.92	
N1097	3	46	24.82	32.47	12.4	6.77	332.5	1 68	82.7	.27	13.40	2.04	+
N1169	3	47	21 73	33.23	23.6	5 77*	416.6	1.37	99 0	.27	19.17	1 38	
N1179	6	32	8.47	24.40	18 2	3.68*	90 7	1.62	39.9	.44	10.71	4.06	
N1232	5	27	34 20	38 57	16.7	9 60*	346.9	1 69	61.2	.28	10.14	2.77	+
N1253	6	57		22.98	17.9	7 88	98.2	3.91	48 8			8.03	+
N1253A	9	53		8.69	19.0	1.11*	4.5	3 85	15.8			24.44	+
N1255	4	47	12 49	19 19	16 9	3 15	88.5	2.24	63.0	.25	7 08	3.56	
N1288	4	21	31 02	32 69	46.7	3.66*	1016.	.90	249.5	12	32.76	.36	
N1309	4	18	14.80	15 54	21.8	2.69		2.92		.18			
N1359	9	32	6 85	11 07	19.6	4.67*	69.4	10.00	148.5	.68	10.13	6.73	
N1365	3	57	43 27	40 81	15 7	11.75	273.8	1.85	43.1	27	6.33	4.29	
N1376	6	17	29.99	26.45	43.4	4 46		1.67		.15			
N1385	6	49	9.03	12 01	14.5	1.60*	23.4	2.91	42 5	.18	2.59	6.85	
N1417	3	50	34 16	34.44	42.9	8.29*	309 8	1 83	68 5	.24	9.07	2 68	
N1418	3	40		19.67	43.9	2.18*	246 8	1.48	167 3			.89	+
N1421	4	76	19.42	17 86	21.3	5.02	91.1	4.13	74.9	.26	4.69	5.51	
N1425	3	62	10.01	19 97	14.3	2 15*	106.8	1.41	70.3	.21	10.67	2.01	
N1507	9	74	1 52	6.34	8.1	.66	37.2	4.33	242 8	.44	24.48	1.78	
N1530	3	55	20 92	49 29	33.1	8.45	367.0	.91	39.6	.40	17.54	2.30	
N1620	4	68	19 87	28.55	36.3	8.56	197.8	2 76	63.7	.43	9 96	4 33	
N1637	5	30	2.53	6 78	6.7	45	43.9	2.55	250.0	.18	17.32	1.02	
N1640	3	43	5.12	12 22	15.3	1.08*	28.3	1.90	49.7	.21	5.52	3.83	
N1642	5	27	27.53	30.51	47.9	6.68*	112.5	1.88	31.7	.24	4.08	5.94	
N1659	4	36	28.54	23.84	47.2	2.77*	112.2	1.28	51.8	.10	3.93	2.47	
N1667	5	36	39.39	21.81	46.7	3.41*	197.8	1 88	109.1	.09	5.02	1.73	+
N1741	9	60	11.48	16.36	36.3	7.07	20.4	6.93	20.0	.62	1.78	34.63	+
N1744	7	54	1.55	10.76	5.9	.55	57.3	1 24	129.9	.35	36.95	.95	
N1784	5	48	13.81	27.32	22.8	7 61	132.9	2 68	46.7	.55	9.63	5.73	
N1800		58	.39	2.45	5.6	.09*	1.0	3.89	42.4	.23	2.49	9.24	+
N1832	4	47	11.00	14.88	18 7	3.71	69 9	4 39	82 7	.34	6.35	5.31	
N1888	5	74	12 26	17.50	24.5	1.43*	150.9	1.23	129.3	.12	12.31	.95	+
N1961	5	47	142.44	64.32	50.1	16 36	2054.	1 04	130 3	.11	14.42	.80	
N1964	3	68	14.52	24 13	15.3	3 68	161.2	1.66	72.6	25	11.10	2.28	
N2090	5	59	1.95	8.70	7 3	1 41	36.7	4 90	127.2	.72	18.81	3.85	
N2139	6	30	9.67	11 33	17 1	4 17	65 7	8 52	134.3	43	6.80	6.35	
N2146A	5	66		17.73	20.8	2.45	29.9	2.04	25.0			8.19	
N2188	9	73	90	4 60	5 3	31	2 4	3 79	30.2	.34	2.70	12 56	
N2207	4	48	46.90	33 44	26.5	11 28	177 7	2 65	41.7	.24	3.79	6.35	+
N2223	3	27	24.42	28.11	26.6	3.26*	520.4	1 08	172.7	.13	21.31	.63	
N2268	4	51	29.67	29.23	29.6	3.24	188.6	.99	57.9	.11	6.36	1.72	
N2276	5	17	39.94	27 03	32.5	4.54		1.63		.11			+
N2280	6	56	14 61	27.98	17.5	13.62*	203 4	4.56	68.2	.93	13.92	6.70	
N2336	4	56	75.97	56.16	28.8	9.48	606.0	79	50 4	.12	7.98	1.57	
N2339	4	40	20.55	21.20	24.4	3 40	217.3	1.98	126.8	17	10.58	1.56	
N2344	5	12	2.64	8 04	12.8	1.00*		4 07		.38			
N2347	3	43	38.70	34 13	56.1	7.11	425.2	1.60	95.8	.18	10.99	1.67	+
N2377	4	27		18.73	23.6	9 11	107 6	6.81	80.4			8.47	
N2388	5	52	6.40	12.86	42.4	5.78*	77.5	9.18	122.9	.90	12.11	7.47	+
N2389	5	38	18.49	26.43	41.4	6.15	261.2	2.31	98.1	.33	14.13	2.35	+
N2441	3	27	28.31	31.08	44.7	4.12*	106.6	1.12	29.0	.15	3.77	3.87	+

Table 2 (continued)

Name	T	i	L_o ($10^9 L_\odot$)	A^o_{25} (kpc)	D (Mpc)	M_H ($10^9 M_\odot$)	M_i ($10^9 M_\odot$)	σ_H (mg. cm^{-2})	σ_i (mg. cm^{-2})	M_H/L_o ($M_\odot/L_\odot$)	M_i/L_o ($M_\odot/L_\odot$)	M_H/M_i (×100)	
1	2	3	4	5	6	7	8	9	10	11	12	13	14
N2525	5	46	7.11	12.31	14.0	.80	44.7	1.39	77.4	.11	6.29	1.79	
N2532	5	32	40.31	35.85	55.1	6.86	240.5	1.40	49.1	.17	5.97	2 85	
N2535	5	55	23.26	34.07	42.2	7.92	29.0	1.79	6.6	.34	1.25	27.31	+
N2541	6	58	1.62	11.93	6.8	1.06	26 1	1.95	48.1	.65	16.08	4.05	
N2552	9	47	.79	5.99	6.8	.29	7.9	2.12	57.5	.37	9.95	3.69	
N2595	5	40	13.64	39.91	44.5	5.39	469.0	.89	77.2	.39	34.37	1.15	
N2608	3	51	7.87	15.49	22.1	.42	21.0	46	23 0	05	2.67	2.00	+
N2613	3	76	28.60	28.09	14.9	3.34	351.4	1 11	116.9	.12	12.29	95	
N2614	5	36	6.17	25.01	30.5	2.36*	239.1	.99	100.3	.38	38.73	99	+
N2633	3	49	14.33	21.19	28.5	3.94*	95.8	2.30	56 0	27	6.68	4 12	+
N2634A	4	79	4.79	12.25	27.5	2.28*	19.9	3.98	34.8	.48	4.16	11.44	+
N2642	4	12	38.59	31.01	43.4	3.47		.95		09			
N2701	5	47	13.88	17.24	29.3	5.36*	64.8	4.73	57.2	.39	4.67	8.28	
N2712	3	55	9.09	17.63	22 5	2.46*	96 8	2.07	81.7	.27	10.65	2.54	
N2735	3	69	3.12	7.52	25.3	2.57	44.1	11.91	204.5	.82	14.13	5 82	+
N2763	6	24	5.59	12.16	17.4	1.33	102.4	2.37	181.6	.24	18.32	1.30	
N2776	5	21	27.18	28.21	32.6	10 24	250 3	3.38	82.5	.38	9.21	4.09	
N2793	9	34	5.17	7.66	20.2	1.34	18.0	5 98	80.5	.26	3.48	7.43	
N2799	9	73	2.25	9.17	21.6	1.29*	33.5	4.01	104.4	.57	14 86	3.84	+
N2805	7	38	24.07	41.44	22.7	15.04	28.9	2.30	4.4	.62	1.20	52 04	+
N2815	3	71	14.63	21.83	23.9	2.47*	258 2	1.36	142.1	17	17.65	96	
N2889	5	27	21.86	20.00	32.6	3.09*	703.9	2 03	461.5	.14	32.20	44	
N2919	3	69	7.46	11.32	24.1	.91*	47.7	1.86	97.7	.12	6 40	1.91	
N2935	3	34	15.91	22 88	21 2	4.97*	228.2	2 49	114.4	.31	14 34	2 18	
N2942	5	36	43.37	35 01	54.1	10.01	217 0	2 14	46.5	.23	5.00	4.61	
N2967	5	17	7.30	16.16	17.8	4.71*		4.73		.65			
N2989	4	41	16.42	17 19	41.5	6.77	191.7	6.01	170.2	.41	11.67	3.53	
N2990	5	56	9.56	10.86	30.9	2.18*	40.4	4.84	89.9	23	4.23	5.39	
N3001	4	47	11.14	21 24	23.1	4.38	196.7	2.55	114.3	39	17 65	2.23	
N3003	4	76	11.20	23.76	17 7	5.98	54.9	2.78	25.5	.53	4.91	10.89	
N3021	4	53	4.10	8.53	18.5	91	26.8	3.30	96.6	.22	6.53	3.41	
N3041	5	49	4.56	13.86	13.6	.98*	67 9	1.34	92.8	.21	14.90	1.44	
N3044	5	84	5.02	11.63	11.9	1.30	45 5	2.52	88.3	.26	9.05	2.85	
N3052	5	43	20.99	21.93	36.3	2.97*	248.0	1.62	135.4	.14	11.82	1.20	+
N3054	3	50	17.59	25.70	22 8	.72*	114.0	.29	45.3	.04	6.48	64	
N3055	5	52	5.12	10 36	17.4	.85*	39.4	2 07	96.4	17	7.70	2 15	
N3124	4	32	29.50	32.98	34.8	6.26	257.3	1 51	62.0	.21	8.72	2.43	
N3145	4	60	33.41	31.62	36 0	4.71	265.8	1 24	69.8	.14	7.96	1.77	+
N3147	4	27	73.60	44.36	36.7	5.30	749.5	71	99.9	07	10 18	.71	
N3162	4	30	5.73	13.53	14 9	2.35	59.7	3.37	85.5	.41	10.41	3.95	
N3177	3	36	2.60	7.13	14.8	.34	49.3	1 74	253.9	.13	18.95	.68	
N3187	5	64	2.65	15 16	18.2	2.00*	39.1	2.29	44.6	.76	14.77	5.13	+
N3223	3	52	38.81	32.87	27.6	3.53*	282.5	86	68.6	.09	7 28	1 25	
N3254	4	71	7.92	19.73	16.1	2.40	97.9	1.62	65.9	30	12.35	2 45	
N3259	4	55	7.35	14.23	22 3	3.84	55.3	4.97	71.6	.52	7.52	6.94	+
N3270	3	76	40.56	52.53	76.3	21.33*	476 2	2.03	45.3	.53	11.74	4.48	
N3287	7	61	3.31	8.36	15.0	.30	5.7	1.14	21.4	.09	1.73	5.30	
N3294	5	58	11.79	16.66	19.1	1.39	62.1	1 31	58.7	.12	5.27	2 24	
N3320	6	58	11.91	17 02	29.1	2.74	90.8	2 48	82.2	.23	7.63	3.01	
N3338	5	48	12.33	22.27	14.7	7.25	162.4	3 84	85.9	.59	13.17	4.47	
N3346	6	27	4.85	11.64	14.1	.73	49.5	1 41	96.0	.15	10.21	1 47	
N3367	5	25	34.61	24.85	35.9	5.07*	251.5	2.15	106.8	15	7.27	2.02	
N3370	5	54	5.12	12.02	14.5	1.67	43.9	3.02	79.7	33	8.57	3 80	
N3389	5	57	4.46	10.20	14.4	.84*	28 7	2 11	72.4	.19	6.42	2.92	
N3433	5	25	22.66	33.38	31.8	6.93	518.9	1 63	122.2	.31	22.90	1.34	
N3445	9	21	9.19	12.41	25.9	2.58*	54.1	4.40	92.1	.28	5.88	4.78	
N3447	8	52		11.94	11.8	1.44*	10.5	2.65	19 3			13.73	+
N3455	3	50	2.14	9.19	12.1	1.59	34.8	4.95	108.0	.75	16.29	4.58	+
N3464	4	46	21.76	29.63	36.7	5.69*	208.1	1.70	62.2	.26	9.56	2.73	
N3511	5	67	4.67	12 22	9.0	2.06*	41.4	3.63	72.8	.44	8.87	4.98	+
N3512	5	25	3.11	8.16	16.3	33	32.1	1.30	126.3	.11	10.32	1.03	+
N3513	5	34	3.23	8 06	9 9	1.08*	17.3	4.36	69.7	.33	5.35	6.26	+
N3521	4	60	14.31	20 25	8.1	2.93	153 9	1.88	98.5	.20	10.75	1.91	
N3549	5	68	25 45	28 70	36.2	7.98*	186 1	2.54	59 3	.31	7.32	4.29	
N3568	5	74		13.23	22.8	2 73*	28.7	4.09	43.0			9.52	+
N3583	3	46	19 28	21.41	27 0	3.96*	166 4	2.26	95.2	.21	8.63	2.38	+
N3596	5	12	7.03	16.71	13.4	1 22		1.15		.17			
N3642	4	32	20 55	35.43	20 9	4 83	27.2	1.01	5.7	.24	1.32	17.76	
N3666	5	73	3.46	11.23	11.6	1 19*	26.4	2.47	54.8	.34	7.61	4.52	
N3672	5	59	19 29	21 78	20.4	7.74	176.8	4.28	97.8	.40	9.16	4.38	-
N3675	3	58	7 52	15 36	9.9	1.28	115.7	1.42	128.7	.17	15.39	1.11	
N3687	4	0	12.25	18.99	30.7	2.69		1.96		.22			
N3689	5	44	12 92	15.00	33.1	1.11*	55.0	1.29	64.1	.09	4.26	2.01	
N3756	4	58	8.92	19.56	16.9	1.13	70.0	.78	48.0	.13	7.85	1.62	+
N3780	5	34	22.87	27.91	31.0	3.44	214.0	1.16	72 1	.15	9.35	1.61	+
N3800	3	75	16.55	19.26	38.9	2.30*	120.5	1 63	85.2	.14	7.28	1.91	+
N3887	4	36	7 05	11 96	12.3	2.07	69.1	3.80	126.8	.29	9.80	3.00	
N3930	5	38	1.23	12.22	11.2	.73*	20.3	1.29	35.7	.60	16.58	3.61	
N3956	5	71	7.41	14.82	17.8	2.16*	35.3	2.58	42.1	.29	4.76	6.13	
N3963	4	25	35 38	34.26	40 6	6.78	185 4	1.52	41.4	.19	5.24	3.66	+
N3976	3	71	25 07	27.32	29.3	9.33	190.6	3.28	67.0	.37	7.60	4.90	+
N4027	8	38	14.37	15 25	18.0	4.04*	34.9	4.55	39.3	.28	2.42	11.58	+
N4030	4	41	18.86	19.64	16.1	4 18	163.2	2.84	111.0	.22	8.65	2.56	
N4037	3	30	1.90	8.11	10.3	.11*	10.3	.42	41.0	.06	5.43	1.03	
N4047	3	30	20 17	19 18	42.9	3.62*	319 4	2.58	227.8	.18	15.83	1.13	+
N4094	5	66	5.25	16.13	15 5	2.58*	48.3	2.60	48.7	.49	9.19	5.35	
N4162	4	52	22.92	21.11	31.0	2.68	123.6	1.58	72.8	.12	5.39	2.17	
N4246	5	55	19.10	30.17	45.0	12.40	191.2	3.57	55.1	.65	10.01	6.49	+
N4254	5	27	104.47	46 08	29.2	19.28	503.3	2.38	62.2	.18	4.82	3.83	
N4273	5	48	18.08	17.94	28.4	2.95	80.5	2 41	65.6	.16	4.45	3.67	+
N4357	4	68	30.73	47.86	51.3	4.62*	474.0	.53	54.3	.15	15.43	.98	
N4388	3	78	47 00	35.11	30.5	1.31	225.6	.28	48.0	.03	4.80	.58	
N4428	5	63	12.48	17.38	34.9	3 85*	64 0	3.34	55.6	.31	5.13	6.01	+
N4485	10	44	1.28	4 99	7.5	.31	8 8	3.25	92.4	.24	6.85	3.52	+
N4561	8	34	3.40	7 29	16.8	1 54	13.3	7.57	65.6	.45	3.91	11.54	
N4595	3	49	.53	3.64	7.2	.10	4.6	1.94	92.1	.19	8.83	2.11	
N4632	5	66	11 59	15.48	19.7	4.30*	29 1	4.70	31.8	.37	2.51	14.78	
N4712	4	63	28 78	36.47	54.4	10 06	395.7	1.98	78.0	.35	13.75	2.54	+
N4814	3	42	19.65	30.07	32.2	5 91*	326.8	1.71	94.8	.30	16.63	1.81	
N4868	3	18	34.83	28.97	58.0	3 56*		1.11		.10			+
N4902	3	21	32 29	27.83	30.5	9.38*	478.7	3.18	162.2	.29	14.82	1.96	
N4939	4	58	67 69	55.79	36.5	14.59	590.5	1.23	49.8	.22	8.72	2.47	
N4951	6	67	3 54	10.65	13.0	1.60	27.7	3.70	64.1	.45	7.81	5.78	
N4961	6	44	6.01	15.22	31.4	2.44	48.3	2 77	54.7	.41	8.04	5.06	+
N4981	4	38	13.41	15.39	19 3	2.18	69.1	2.41	76.5	.16	5.15	3.15	
N5000	4	30	24 90	38 68	69.3	6.25	142.9	1.10	25.1	.25	5.74	4.37	
N5005	4	61	17 68	17 13	12.4	.29	190.6	.26	170.3	.02	10.78	.15	
N5012	5	53	21 73	25 27	32 5	4 57*	253 3	1 88	104 1	.21	11.66	1.80	

Table 2 (continued)

Name 1	T 2	i 3	L_o ($10^9 L_\odot$) 4	A_{25}^o (kpc) 5	D (Mpc) 6	M_H ($10^9 M_\odot$) 7	M_i ($10^9 M_\odot$) 8	σ_H (mg. cm^{-2}) 9	σ_i (mg. cm^{-2}) 10	M_H/L_o ($M_\odot/L_\odot$) 11	M_i/L_o ($M_\odot/L_\odot$) 12	M_H/M_i (×100) 13	14
N5016	5	40	13 09	17.00	32 0	2.79*	143.5	2.53	130.2	21	10.97	1.95	
N5054	4	53	21 01	26.87	19.6	1.78	150.9	.65	54.9	.08	7.18	1.18	
N5079	4	55		15.08	33.6	1.15*	44 1	1 33	51.0			2.61	+
N5088	3	73	3.29	10.24	15.9	2.57*	21.5	6.43	53.8	.78	6.54	11.96	
N5134	3	54	9.34	14.93	19.7	.63*	13.2	.74	15.5	07	1.41	4 75	
N5169	3	66	3.77	18.67	31.0	2.91*	32.7	2.19	24.6	.77	8.67	8.90	+
N5172	4	56	48.29	43.66	49.4	12.16	381.0	1.67	52.4	.25	7.89	3.19	
N5247	4	30	15.37	23.86	14.9	3.48	56.3	1.60	25.9	.23	3.66	6.18	
N5258	3	45	67.07	41.76	82.8	13.20*	455.4	1.98	68.5	.20	6.79	2.90	+
N5293	5	34	21.06	40.28	71.0	6.71	491.5	1.09	79.5	.32	23.33	1.37	+
N5297	4	79	26.24	38.33	30.9	1.70	213.2	.30	38.1	.06	8.12	.80	+
N5301	3	80	13.71	18.87	19.7	4.96	83.3	3.66	61.4	.36	6.07	5.96	
N5313	3	53	11.57	16.74	32.4	3.08	141 8	2.88	132.8	.27	12.25	2.17	
N5324	5	12	26.44	26.52	36.4	5.99*		2.23		.23			
N5350	3	38	17.94	26.29	28.2	4.42*	217.0	1.68	82.3	.25	12.10	2.04	
N5351	3	56	27.56	37.44	45.4	9 62	350.3	1.80	65.6	.35	12.71	2.75	+
N5356	4	74	2.71	12.34	16.6	.30*	13.6	.51	23.4	.11	4.99	2 19	
N5364	4	46	16.48	29.25	14.7	2.67	146.5	.82	44.9	16	8.89	1 82	+
N5371	4	34	54.62	41.12	32.5	7.37	664.4	1.14	103.1	.13	12.16	1.11	
N5395	3	57	41.62	36.24	44.2	8.51	577.0	1.70	115.3	.20	13.86	1.47	+
N5464	10	48	12.38	9.08	31.3	4.23*	20.0	13.46	63.6	34	1.62	21.17	
N5468	6	12	28.22	25.89	34.0	7.38		2.89		.26			
N5480	5	47	8.57	12.60	24.9	.82	21.8	1.36	36.1	.10	2.55	3.77	+
N5486	9	49	2.01	8.75	18.9	.79	14.0	2.72	47.9	.39	6.94	5.67	
N5545	4	70		11 90	39.2	2.25	54.2	4.16	100.3			4.15	+
N5584	6	40	13.07	18.78	19.7	2 48	69.5	1.84	51.7	.19	5.31	3.57	
N5595	5	54	19.14	17.86	31.9	7.83*	75.1	6.44	61.7	.41	3.92	10.43	+
N5600	5	12	9.62	12.52	29.1	1.49*		2.50		.15			
N5633	3	52	19.67	22.98	36.7	3.06	116.6	1.52	57.9	.16	5.93	2.63	+
N5645	7	50	4.41	11.69	16.6	1.43	25.5	2.74	48.9	32	5.78	5.61	
N5653	3	32	25.62	23.65	44.3	5.34	375 9	2.51	176.3	.21	14.67	1.42	
N5660	5	25	21.25	25.43	30.4	5.90	77.5	2.39	31.4	.28	3.65	7.61	
N5665	5	46	11.66	16.00	27.1	.95*	39.6	.98	40.6	.08	3.40	2.40	+
N5669	6	40	9.47	20.13	17.2	2 59	60.0	1.68	38 9	.27	6.34	4.32	
N5672	3	49	8.06	12.48	44.9	3.24*	38.7	5.45	65.1	.40	4.80	8.37	
N5676	4	60	35.99	28.50	28.0	6.99	235.6	2.26	76.1	.19	6.55	2.97	
N5678	3	60	21.35	22.13	25.9	4.52*	153.5	2.42	82.2	.21	7.19	2.94	
N5682	3	76	3.71	13.80	30.0	1.12*	21.7	1.54	29.9	30	5.84	5.16	+
N5690	5	72	10.81	18.08	21.3	3.28*	56.4	2.63	45.3	.30	5.22	5.82	
N5693	7	32		16.52	29.9	1.31	8.0	1.26	7.7			16.36	+
N5740	3	57	7.44	15.95	19.0	2.66	85.5	2.74	88.2	.36	11.49	3.11	+
N5746	3	83	43.61	34.96	20.2	3 03	699.9	.65	150.3	07	16.05	.43	
N5792	3	76	30.94	39.85	23.4	7.62	232.2	1.26	38.4	25	7.51	3.28	
N5806	3	58	5.38	12.03	14.3	.51	58.0	.93	105.1	.10	10.78	.88	+
N5829	5	27	12.11	35.12	60.6	6.02	179.8	1.28	38.2	.50	14.84	3.35	+
N5832	3	51	.83	8.97	8.0	53	14.4	1.71	47.1	.63	17.43	3.64	
N5850	3	25	30.65	35.15	26.8	2.09	248.6	.44	52.8	.07	8.11	.84	+
N5861	5	55	14.21	18.72	22.4	3 53*	91.5	2.64	68.5	.25	6.44	3.86	+
N5874	4	44	6.97	24.60	34.6	3.03	217.4	1 32	94.2	.44	31.18	1.40	
N5899	5	65	15.76	20.93	27.8	3.91	214.1	2.34	128 2	.25	13.58	1.82	+
N5900	3	71	2.35	11.12	28.4	5.06*	113.7	10.72	241.1	2.16	48.47	4.45	+
N5905	3	38	32.68	45 47	37.5	19.62	464.5	2.49	58.9	.60	14.21	4.22	
N5954	6	60	3.34	7.29	21.5	1.01	46.5	4.99	229.1	.30	13.92	2.18	+
N5962	5	43	14.38	17.45	21.5	1.66	142.1	1.43	122.4	.12	9.88	1.17	
N5964	7	36	2.19	19.40	15.8	2.10	65.9	1.47	46.0	.96	30.04	3.19	
N5970	5	46	13.65	18.10	21.4	1.93	98.9	1.55	79.2	.14	7.24	1.95	+
N5981	5	82	32.53	32.50	55.0	7 88*	182.9	1.96	45.4	.24	5.62	4.31	+
N5985	3	55	34.56	42.92	28.7	2.70	478.8	.39	68.2	.08	13.85	.57	+
N6015	6	65	5.83	14.73	10.9	2.61	69.1	3.15	83.6	.45	11.85	3.77	
N6032	3	62	6.46	22.80	47.5	4 72*	109.8	2.38	55.4	.73	16.99	4.30	
N6070	6	56	13.99	21.84	21.6	3.52	144.7	1.94	79.6	.25	10.35	2.43	
N6106	5	55	4.99	11.68	16.3	1.99	38.0	3.83	73.0	.40	7.61	5.25	
N6118	6	62	14.02	21.39	16.9	2 27	110 5	1.30	63.4	.16	7.88	2.05	
N6140	5	41	3.44	21.46	12.0	3.50	81.2	1.99	46.3	1 02	23.62	4.31	
N6181	5	61	16.66	18.02	26.5	4.04	107.0	3.26	86.4	.24	6.42	3.77	
N6217	4	30	15.44	18.68	19.7	5.93	120.2	4.46	90.3	.38	7.79	4.94	
N6239	3	62	2.36	8.55	11.9	1.30	17.4	4.66	62.3	.55	7.35	7.49	
N6315	5	32	24.08	20 58	73.1	9 61*	229.2	5 96	142.0	.40	9.52	4.20	+
N6372	3	47	16.27	28.81	52.1	4.45	153.0	1.40	48.4	.27	9.41	2.90	
N6381	4	40	10.95	16 82	37.0	3.02*	104.0	2.80	96.4	.28	9.49	2.90	+
N6384	4	46	33.23	35.54	18.9	9.74	347 2	2 02	72.1	.29	10.45	2.80	
N6412	5	27	9 66	13.89	19.3	1.75	30.3	2.38	41.2	.18	3.14	5.78	
N6491	3	67	15 72	20.66	59.2	11.69*	136.7	7.18	84.0	.74	8.70	8.55	+
N6555	5	36	15 29	17.23	25.5	1.44	74 0	1 27	65.4	.09	4.84	1.95	
N6570	9	52	17.36	13.67	26.0	1.73	41.2	2.43	57.9	.10	2.37	4.19	
N6574	4	38	16.03	12.32	26.2	.83	187.9	1.44	324.9	.05	11.72	.44	
N6621	5	62	48 40	37.60	68.8	10.37*	237.0	1.92	44.0	.21	4.90	4.37	+
N6627	3	21	25.30	31 16	57.6	4.63*	27.0	1.25	7.3	.18	1.07	17.16	
N6632	4	61	10.45	21.57	25.0	1.60*	169 1	.90	95.3	.15	16.18	.95	
N6643	5	59	18.07	19.85	18.5	7.15	220.8	4.76	147.0	.40	12.22	3.24	+
N6674	3	55	34.89	48.43	38.6	24.58*	465.7	2.75	52.1	.70	13.35	5.28	
N6690	7	69	1 71	7.46	7.8	.53*	12.7	2.49	59.6	.31	7.39	4.18	
N6764	3	54	13.95	20.48	28.6	3.23	100.5	2.02	62.9	.23	7.21	3.21	
N6814	4	18	17.83	19.81	17.9	3.40		2.28		.19			
N6821	7	30		6.56	17.7	1.39	23.0	8.45	140.2			6.03	
N6836	9	17		7.27	18.6	2.15		10.70					+
N6906	4	61	38.58	27.49	53.2	7.44*	261.7	2.58	90.9	.19	6.78	2.84	
N6907	4	30	47.47	36.46	34.3	19.73	588.6	3.89	116.1	.42	12.40	3.35	
N6923	3	57	17.48	20.93	30.1	9.91*	166.2	5.94	99.5	.57	9.51	5.97	
N6925	4	69	37.87	31.34	29.9	14.03	311.5	3.75	83.2	.37	8.22	4.50	
N6951	4	30	18.14	23.24	18 0	2 78	361.5	1.35	175.6	.15	19.92	.77	
N7015	4	27	51.08	34.87	53.8	7.02*	187.8	1.52	40.5	.14	3.68	3.74	
N7080	3	18	21.74	35.64	53.8	6.54		1.35		.30			
N7102	3	50	24.60	28.57	53.2	6.87*	75.1	2.21	24.1	.28	3.06	9.14	
N7137	5	25	6.13	10.17	21.0	1.38	64.2	3.49	162.9	.22	10.48	2.14	
N7156	6	24	13.48	22.59	43.9	2.04	61.2	1.05	31.5	.15	4.54	3.34	
N7171	3	52	13.03	22.99	29.8	7.17*	160.0	3.56	79.5	.55	12.28	4.48	+
N7177	3	47	8.92	14.56	15.0	1 34*	90.9	1.66	112.5	.15	10.19	1.48	
N7184	5	74	45.21	38.62	28.5	11.19*	411.2	1.97	72.3	.25	9.09	2.72	
N7292	10	36	2.45	8.29	13.3	.83*	11 4	3.19	43.7	.34	4.67	7.29	
N7298	5	27		21 44	47.4	4.24	109.4	2.42	62.4			3.87	+
N7300	3	59	20.52	27.60	47.2	8.44*	230.9	2.91	79.5	.41	11.25	3.66	+
N7309	5	17	17.40	24.61	38.0	2.20*		.95		.13			
N7319	4	40	33.49	38.20	72 5	7.32	80.0	1.32	14.4	.22	2.39	9.15	+
N7339	4	75	4.93	11.95	16.7	.64	33.6	1.17	61.8	.13	6.82	1.90	
N7343	4	34	21.90	25.27	66.7	3.92*	84.4	1.61	34.6	.18	3.85	4.64	+
N7392	4	53	15.93	16.56	29.6	2.88	90.3	2.76	86.4	.18	5.67	3.19	
N7393	5	61		19.35	36.4	3.66*	62.5	2.56	43.8			5.85	
N7416	3	73	10.84	22.49	27.6	1 95*	98.2	1.01	51.0	.18	9.06	1.99	
N7418	6	34	6.01	12.91	13.3	.88	45.4	1.39	71.4	.15	7.55	1.94	+
N7460	3	38	5.58	11.64	31.6	3 35*	282.8	6.48	547.9	.60	50.69	1.18	
N7479	5	38	25.66	28.42	24.0	5.67	409.8	1.84	133.1	.22	15.97	1.38	
N7513	3	38	4.02	14.00	14.8	.16*	58 3	.22	78.0	.04	14.51	.28	
N7537	4	77	5.33	13.94	26.1	5.85	58.0	7.91	78.4	1.10	10.87	10.09	+
N7541	4	68	16.64	22 52	26.3	11.57	151.5	5.98	78.4	.69	9.10	7.64	
N7606	3	66	26.54	32.11	22.0	4.13*	409.6	1.05	104.2	.16	15.43	1 01	
N7664	5	56	15.06	30.33	34.5	10.58	176 4	3.02	50.3	.70	11 71	6 00	
N7678	5	41	18.50	23.03	34.0	4.35	108.5	2.15	53.6	.23	5.86	4.01	
N7713	7	63	2.05	7.07	6.5	.38	9.3	2.01	48.8	.19	4.55	4.11	+
N7716	3	32	8.17	16.97	25.1	2.31*	116.2	2.10	105.8	.28	14.22	1.99	
N7721	5	64	10.25	16.93	19.7	5.40*	70.1	4.94	64.2	.53	6.84	7.70	
N7723	3	45	12.39	19.12	18.6	1.05*	460.7	.75	330.7	.08	37.17	.23	
N7741	6	45	3.06	10.17	9.0	.82	22.9	2 09	58.0	.27	7 46	3.61	
N7742	3	12	6.60	10.63	17 0	56		1.30		.08			
N7750	6	57	6.70	13.40	28.4	4.43	59.2	6.47	86.5	.66	8.83	7.48	
N7753	4	50	34.08	47.52	49.7	13.43	412.9	1.56	48.0	.39	12.12	3.25	+
N7755	5	38	22.62	29.31	27.3	7.09*	356.4	2.15	108.9	.31	15.75	1.98	
N7757	5	21	6.25	22.01	28.6	2.67	225.3	1.45	122.0	.43	36.03	1.19	
N7769	3	12	23.95	22.73	40.7	2.84		1 44		.12			+
N7782	3	55	32.58	33.14	51.0	4.20	462.0	1.00	110.4	.13	14.18	.91	
N7816	4	27	16.83	28.75	49.6	4.43*	183.5	1.41	58.2	26	10.90	2.41	
N7817	4	74	15.26	20.16	23.1	1.86	134.1	1.20	86.6	12	8.79	1.39	
I 167	5	49	5.20	23.21	28.3	6 59	26.8	3.21	13.0	1.27	5.15	24.61	+
I 467	5	65	18.90	24.59	27.7	3.29*	80.2	1.43	34.8	.17	4.24	4.11	
I1029	3	82	15.09	20.04	31.3	6.47	154.3	4.23	100.8	.43	10.23	4.19	
I1291	8	32	3.17	14.95	23.5	2.80*	70.4	3.28	82.6	.88	22.21	3.97	
I1301	6	43	9.24	19.40	45.0	6.94	92.4	4.84	64.4	.75	9.99	7.52	
I1302	5	44	28.73	16.97	52.0	6.27*	332.9	5.71	303.4	.22	11.59	1.88	+
I1303	5	48	10.52	24.26	49.9	2 35*	114.6	1.05	51.0	.22	10.89	2.05	+
I1401	3	67	14.00	29.24	51.8	6 63	143.8	2.03	44.1	47	10.27	4.61	
I1417	3	75		15 73	46.8	11.26*	163.5	11.93	173.3			6.89	+
I1738	3	38		5.84	16.4	2.47*	92.8	18.95	713.3			2.66	+
I1746	3	72	1.96	10.80	24.1	.57*	78.7	1 27	177.0	.29	40.13	.72	+
I1953	7	36	9.49	16.20	19.9	1.84*	434.1	1.83	434.0	.19	45.74	.42	+
I2163	5	64		18.70	26.0	6.48*	19.1	4.86	14.3			33.88	+
I2166	5	44	13.86	26.51	34.5	4.57*	207.8	1.70	77.6	.33	14.99	2.20	
I2233	7	87	.86	6.38	7.2	.67*	7.3	4.29	46.9	.77	8.45	9.16	
I2389	3	83	10.90	11.56	31.3	3.61*	11.6	7.10	22.8	33	1.07	31.13	+
I3576	9	17	.41	8.72	12.0	.45		1.56		.11			
I4351	3	83	48.17	38.07	30.7	13.65*	286.2	2.47	51.8	.28	5.94	4.77	
I5039	7	74	12.73	16.78	29.1	14.75*	35.4	13.74	32.9	1.16	2.78	41.71	+
I5264	3	90		8.75	18.9	1.54*	.8	5.28	2.7			193.76	+
I5271	3	69		11.65	15.9	.92*	55.0	1.78	106.2			1.68	
I5273	6	43	5.01	9.84	12.0	.94*	34.3	2.54	93.0	.19	6.84	2.74	
A 26 +0240	3	77		10.11	42.4	4 46*	35.8	11.46	91.9			12.48	+
A 102 -0628	7	27	2.78	12.60	10.8	2.47	65.2	4.08	107.8	.89	23.47	3.79	
A 115 +1107	6	48	13.75	34.63	48.8	5.40*	215.4	1.18	47.1	.39	15.67	2.51	
A 135 +0716	6	38	6.00	26.17	40.8	2.37*	61.7	.91	23.6	.40	10.29	3.85	
A 139 +1343	10	70	23.00	39.40	49.6	9.28*	24.9	1 57	4.2	.40	1.08	37.25	+
A 140 +1254	10	45	13.29	29.34	49.8	5.49*	30.1	1.67	9.2	.41	2.26	18.24	+
A 509 -1451	5	34	6.87	16.29	19.3	1.84*	84.6	1.81	83.6	27	12.31	2.17	
A 609 +7109	3	36	13.98	37.35	52.1	12.26	604.3	2.31	113.6	.88	43.22	2.03	+
A 628 +6343	3	76	38.60	23.46	48.9	7.10*	113.0	3 38	53.9	.18	2.93	6.28	
A 705 +7155	3	90	42 60	24.46	39.7	12.44	84.0	5 46	36 8	.29	1.97	14.81	
A 705 +1515	5	61	7.66	15.09	22.0	1.72*	33.8	1 98	39.0	.22	4.41	5.09	
A 713 +2957	5	82	9.32	15.08	33 4	4.88*	39.5	5.63	45.6	.52	4.24	12.35	
A 717 +7141	5	46	21.70	21.50	37.8	4.78*	140.2	2.71	79.6	.22	6.46	3.41	
A 756 +1634	5	25	6.46	23.95	50.5	3.81	185.2	1.74	84.7	.59	28.68	2.06	
A 949 +4305	3	55	15.37	38 13	58.9	9.71*	121.5	1.75	21.9	.63	7.91	8.00	
A1113 -3341	3				33.3	1.07*							+
A1144 -0334	3	52		20.82	61.7	5.58*	23.7	3.38	14.3			23.60	+
A1308 +0340	5	88	5.43	10.52	36 4	4.02	11.4	9.53	27.1	.74	2.11	35.11	
A1930 +5400	3	38	12.22	27.79	43.6	5.17	282.6	1.76	96.0	.42	23.12	1.83	
A2148 +2537	3	21	12.22	32.01	62.8	11.75	439.1	3 01	112.4	.96	35 94	2.68	
A2255 +0202	5	27		23.91	46.2	3.66	120.6	1.68	55.4			3.03	
A2339 -0356	5	80		22 41	65 8	4.89*	33.5	2 56	17.5			14.59	+
A2346 +0552	6	0		5.97	36.6	1.32*		9.76					

Column 1: Identification of the galaxy (NGC, IC, A)
Column 2: Morphological type according to the RC2
Column 3: Inclination of the galaxy upon the plane of the sky
Column 4: Intrinsic luminosity reduced to the galactic pole and zero inclination and redshift
Column 5: Linear diameter at the 25 mag arc sec^{-2} brightness level reduced to the galactic pole and zero inclination
Column 6: Distance calculated using H_0^* from de Vaucouleurs and Bollinger (1979)

Column 7: Mass of neutral hydrogen
Column 8: Indicative total mass
Column 9: Neutral hydrogen surface density
Column 10: Indicative total mass surface density
Columns 11–13: Ratios of the previous parameters
Column 14: a + indicates a note given in the companion paper (Bottinelli et al., 1982b)

* New determination

---

hydrogen mass, indicative total mass) have been calculated using both sets of distance determinations for each of the five type classes by including the same galaxies in both cases. The dispersion in each class (Table 1) for each of these four parameters decreases when the distances given by de Vaucouleurs are used. A similar decrease is observed for the dispersion of the relations between M_H, M_i, L_0, and A_{25}^0. It appears thus that a *constant* Hubble flow is not the best choice that can be made for evaluating distances for our sample of galaxies.

In order to take into account the anisotropy of the Hubble flow the description given by de Vaucouleurs and Bollinger (1979) has been adopted. Thus the Hubble ratio H_0^* depends on supergalactic coordinates SGL and SGB in the following way:

$H_0^* = 81.2$ for SGB $\leq 30°$ and $0° < \text{SGL} \leq 180°$

$H_0^* = 108.8$ for SGB $\leq 30°$ and $180° < \text{SGL} < 360°$

$H_0^* = 95.1$ for SGB $> 30°$ and $0° \leq \text{SGL} \leq 360°$,

where H_0^* is expressed in km s^{-1} Mpc^{-1}.

The previous test was repeated by calculating the distances, first from V_0/H_0^* and then from $V_0/100$ for the same galaxies (i.e. the whole sample in the present case). The results given in Table 1 show that the dispersion is smaller when using H_0^* instead of $H_0 = 100$. The decrease of the dispersion is significant though it is small.

Thus the integral optical and H I parameters will be calculated using the distance $D = V_0/H_0^*$. However better results are expected from better distance determinations such as those obtained from the Tully-Fisher relation (Bottinelli et al., 1980c).

Before calculating the integral parameters the problem of H I self-absorption has to be discussed. Heidmann et al. (1972) gave a correcting term C_F on the H I flux F_H, depending on the inclination i of the polar axis of the galaxy to the line of sight according to the relation:

$$C_F = F_H(0)/F_H(i) = (0.031/\cos i)/[1 - \exp(-0.031/\cos i)].$$

This correction is generally very small as shown on the histogram (Fig. 4) of C_F values for our sample.

The test previously used was performed by calculating the mean value $\langle M_H \rangle$ of M_H for each class of morphological type taking or not into account the self absorption correction (Table 1). It is worth noting that this very small correction induces a decrease of the dispersion of M_H values in three cases (in the two other cases the dispersion remains unchanged) with a population as high as 107 galaxies.

In conclusion, the H I fluxes will be corrected for self absorption using the above factor C_F.

The integral parameters are given in Table 2 for each galaxy of the sample. It must be noted that for inclination i smaller than 20° the line width and consequently the indicative total mass M_i are not given, because of the large uncertainties.

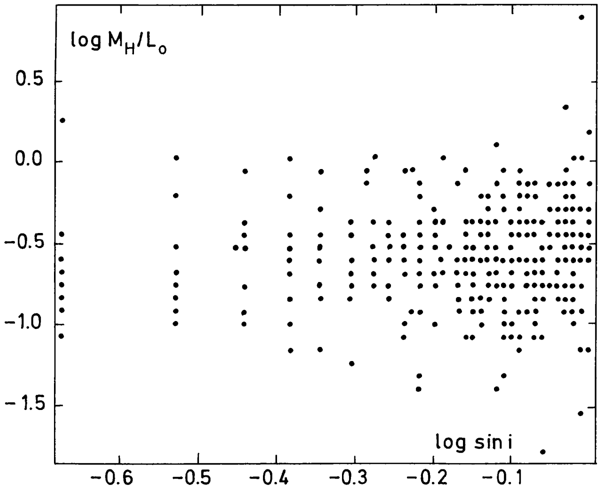

Fig. 5. The corrected H I mass-to-luminosity ratio (in solar units) is plotted against the sine of the inclination, both in logarithmic scale, for all the measured galaxies. No bias with inclination is present

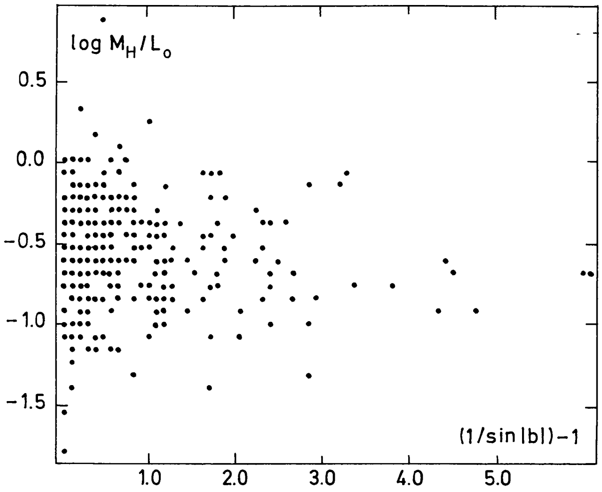

Fig. 6. The corrected H I mass-to-luminosity ratio (in solar units), in logarithmic scale, is plotted against the quantity $(1/\sin|b|) - 1$. No bias with the galactic latitude b is present

---

Before computing mean values of each integral parameter within different morphological types it is necessary to test any possible statistical or observational bias.

IV. Discussion of Possible Biases

The present sample of galaxies can be subject to a variety of selection effects. These may be produced essentially by (i) the corrections for inclination and galactic extinction (ii) the instrumental resolution (iii) a bias reflecting the limitation in magnitude of optical catalogs.

IV. 1. Inclination Effect

In order to test whether corrections for inclination effect are suitable, the independent distance ratio M_H/L_0 was used.

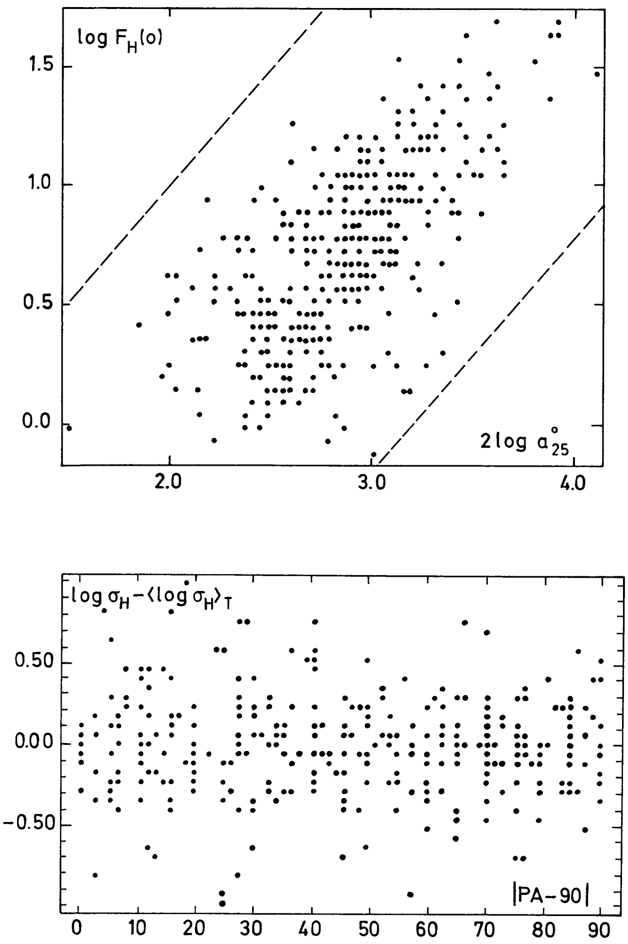

Fig. 7. a The corrected H I flux (in $10^6\,M_\odot\,\mathrm{Mpc}^{-2}$) is plotted against the square of the apparent diameter (in 0'.1 units), both in logarithmic scale, in order to test a possible bias due to the beam size. The relation appears to be linear with a slope equal to 1, indicating that the sample is not strongly affected from this bias. **b** The mean neutral hydrogen projected density σ_H (in logarithmic scale) normalized to the mean value for each morphological type T is plotted against $|PA-90°|$ where PA is the position angle (in degrees) of the major axis. No effect due to the orientation of galaxies is present

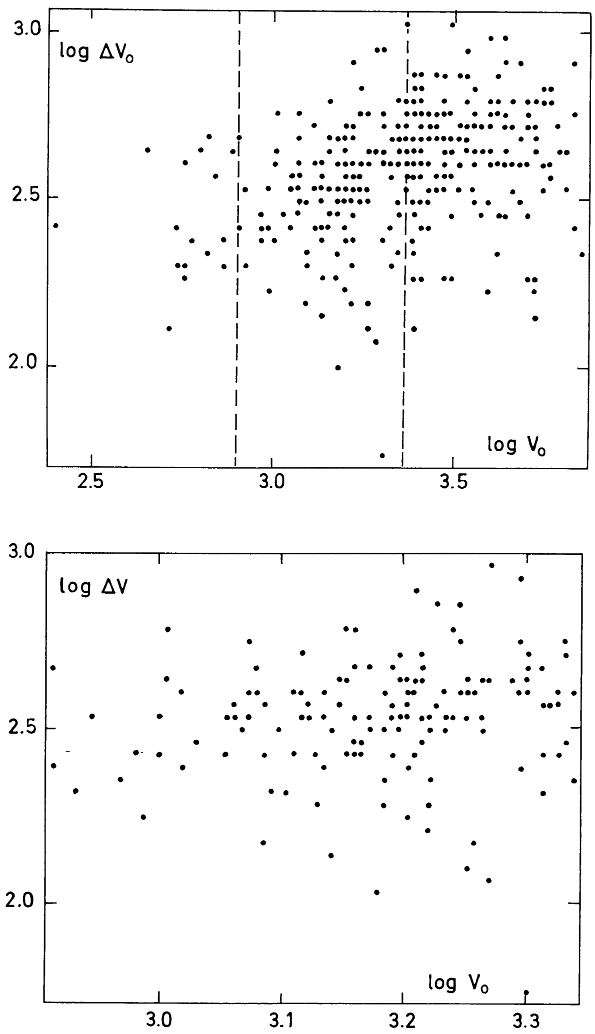

Fig. 8. a The line width ΔV_0 (in km s^{-1}), corrected for bandwidth and inclination effects, is plotted against the systemic radial velocity V_0 (in km s^{-1}), both in logarithmic scale, in order to test a possible Malmquist effect. There is a significant increase of ΔV_0 with V_0. The two cut-off shown in the figure have been used, in order to obviate the bias (see text). **b** Same as **a**, for the restricted sample

log (M_H/L_0), where M_H and L_0 are corrected values, is plotted versus log (sin i) in Fig. 5: no significant effect is present. Because the evaluation of sin i depends slightly on the morphological type (Bottinelli et al., 1980a) this test has been repeated for each morphological type and again no effect is found.

IV. 2. Galactic Latitude Effect

A similar test has been performed versus the galactic latitude b by plotting log (M_H/L_0) as a function of cosec $|b|-1$ (Fig. 6). No significant correlation has been found. This test is just a confirmation that the cosec b law is suitable.

IV. 3. Source-to-beam-size Ratio Effect

A lack of neutral hydrogen could be present for large galaxies because of the relative small size of the beam of the radiotelescope. To obviate this effect galaxies with an E−W apparent diameter larger than 3' have been measured systematically at several adjacent positions on the sky. For smaller galaxies a typical correction factor for beam attenuation C_B can be estimated by assuming a gaussian large-scale H I distribution with an half-intensity H I diameter $\Gamma_{\mathrm{H\,I}}$ along the E−W direction; then, $C_B = [1+(\Gamma_{\mathrm{H\,I}}/4')^2]^{1/2}$. The ratio of H I diameter to optical Holmberg diameter for spiral galaxies in our sample is ≈0.6 (Bottinelli, 1971); thus, $\Gamma_{\mathrm{H\,I}} \approx 0.6\ a_{\mathrm{EW}}$, where a_{EW} is the EW Holmberg diameter. It results that C_B ranges from 1.01 to 1.09 for a_{EW} ranging from 1' to 3'. Note that the uncertainty in the correction could be as large as the correction itself for an individual galaxy; no such correction was applied to the data given in Table 2. In order to test a possible remaining effect, log F_H has been plotted versus 2 log a^0_{25} (Fig. 7a). If no effect is present a linear correlation with a slope equal to 1 is expected. On the contrary, if such an effect is present the correlation is expected to be non-linear or the slope different

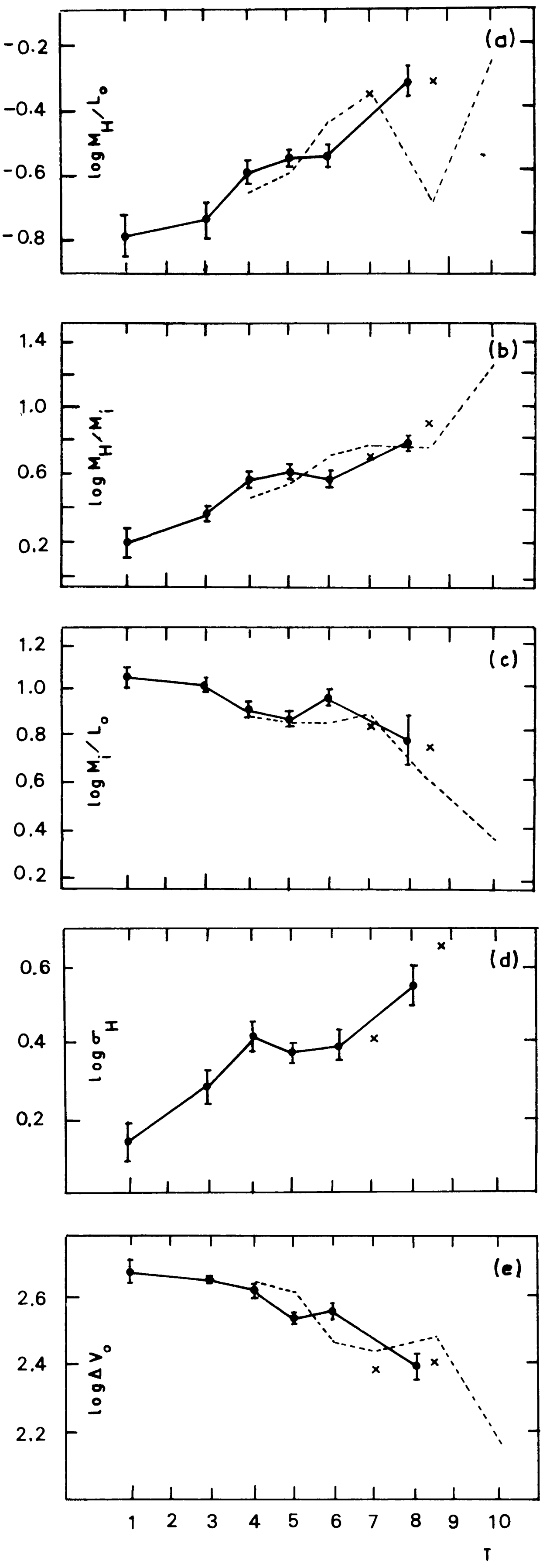

from 1. Figure 7a shows that the relation is quite linear. A Student-test indicates that the slope is not significantly different from 1 (at the 0.01 probability level). However, for a given a_{25}^0 diameter, there could be also an effect due to the orientation of the galaxy. This effect was tested in Fig. 7b where the mean neutral hydrogen projected density σ_H (as defined in Sect. II) is plotted versus the angular separation of the major axis from the EW direction as described, from the position angle PA, by $|PA-90°|$, for 330 galaxies having no uncertain position angle. Figure 7b shows that σ_H does not increase from EW galaxies ($|PA-90|\approx 0$) to NS galaxies ($|PA-90|\approx 90$) as expected if an effect was present. The correlation coefficient of the linear regression obtained by the least-squares method is 0.03 and the slope is not significantly different from 0.

IV. 4. Malmquist Effect

Roberts (1978) has brought to light how a classical selection effect (Malmquist, 1920) occurs when studying log (ΔV_0) versus log V_0. At high velocities there is a bias towards large ΔV_0 because only the most luminous galaxies (i.e. with large ΔV_0) are detected. The plot of log (ΔV_0) versus log V_0 for our sample is displayed in Fig. 8a. Indeed it appears that a lack of faint galaxies (i.e. with small ΔV_0) is present at high velocities. In addition a lack of luminous galaxies (i.e. with large ΔV_0) appears at low velocities. The luminosity function of galaxies is reflected in this effect that implies a poor population of luminous galaxies when restricting to the vicinity of our Galaxy. There appears thus necessary to achieve two cut-off at both low and high velocities. Various limits have been tested and the following limitations have been adopted which gives still a rich sample but without bias:

$$2.90 \leqq \log V_0 \leqq 3.35.$$

These two cut-off are shown in Fig. 8a. Log ΔV_0 is plotted versus log V_0 for the restricted sample in Fig. 8b and there is no more correlation.

There are 152 galaxies belonging to this restricted sample. Their distribution according to morphological type and luminosity class is shown as the hatched region of Figs. 1 and 2.

V. Mean Logarithmic Values of the Integral Parameters

The sample being restricted as stated above it is possible to determine *unbiased* mean values of integral parameters for each morphological type. These values shown in Table 3 are after a 2σ rejection. A comparison with previous data obtained for early type galaxies (Bottinelli et al., 1980a) and for late type (Shostak, 1978) is given in Fig. 9 all the data being reduced to our distance scale. It shows an overall general agreement and confirms a general increase of M_H/L_0 and M_H/M_i, and a general decrease of M_i/L_0

Fig. 9a–e. Mean logarithmic values of the parameters: **a** M_H/L_0; **b** M_H/M_i; **c** M_i/L_0; **d** σ_H; **e** ΔV_0 as a function of morphological type T. The parameters are expressed in the same units as in Table 2. The dashed line shows the data obtained by Shostak. The point corresponding to $T=1$ is taken from Bottinelli et al. (1980a). The point at $T=8$ corresponds to types $\geqq 7$ (the mean being $T=8$). Crosses show the result obtained for $T=7$ alone and $T=8$ and 9 together

Table 3. Mean parameters for each morphological type

Type	3	4	5	6	≥7
log L_0	0.97	1.08	0.87	0.81	0.58
σ, (n)	0.36(32)	0.23(30)	0.24(43)	0.25(19)	0.23(16)
log A_{25}^0	1.20	1.25	1.17	1.14	1.02
σ, (n)	0.22(37)	0.11(28)	0.10(42)	0.17(21)	0.14(23)
log ΔV_0	2.65	2.62	2.53	2.56	2.39
σ, (n)	0.06(23)	0.10(25)	0.09(40)	0.10(21)	0.19(21)
log M_H	0.29	0.50	0.23	0.22	0.20
σ, (n)	0.34(33)	0.16(23)	0.23(40)	0.23(19)	0.16(18)
log M_i	1.96	1.98	1.63	1.70	1.34
σ, (n)	0.37(31)	0.30(27)	0.20(36)	0.26(20)	0.38(20)
log σ_H	0.28	0.41	0.37	0.38	0.54
σ, (n)	0.23(30)	0.20(25)	0.20(46)	0.18(19)	0.27(24)
log σ_i	1.89	1.88	1.80	1.77	1.75
σ, (n)	0.17(29)	0.12(21)	0.16(39)	0.13(17)	0.28(18)
log M_H/L_0	−0.74	−0.60	−0.56	−0.56	−0.33
σ, (n)	0.35(32)	0.20(28)	0.23(42)	0.19(18)	0.22(18)
log M_H/M_i	0.37	0.57	0.61	0.57	0.79
σ, (n)	0.28(30)	0.26(25)	0.18(38)	0.23(21)	0.18(17)
log M_i/L_0	1.00	0.89	0.86	0.95	0.78
σ, (n)	0.17(28)	0.18(27)	0.20(39)	0.13(17)	0.48(18)

For each parameter (defined in the same units as in Table 2), the mean logarithmic value (first line) within a morphological type, the r.m.s. dispersion and the number of data in parentheses (second line) are given. The sample is restricted to the unbiased velocity range: $2.90 \leq \log V_0 \leq 3.35$; ΔV_0 and M_i are not calculated for inclinations smaller than 20°. All values are after 2σ rejection

Table 4. Influence of companions on the mean ratio M_H/L_0

Type (1)	all sample (2)	no companions (3)	with companions (4)
3	−0.74	−0.65	−0.79
	0.35(32)	0.15(11)	0.41(21)
4	−0.60	−0.56	−0.68
	0.20(28)	0 15(19)	0.27(9)
5	−0.56	−0.51	−0.63
	0.23(42)	0.17(25)	0.29(17)
6	−0.56	−0.55	−0.60
	0.19(18)	0.19(14)	0.21(4)
≥7	−0.33	−0.30	−0.35
	0.22(18)	0.26(6)	0.21(12)

For each morphological type (Column 1), the mean logarithmic value of M_H/L_0 (first line), the r.m.s. dispersion and the number of data in parentheses (second line) are given, from the following samples:
(i) All galaxies are considered (Column 2)
(ii) Galaxies with companions are excluded (Column 3)
(iii) Only galaxies with companions are considered (Column 4)

and ΔV_0 when going from early to late types. Our results show also a systematic increase of the mean H I projected density σ_H along this sequence, which confirms also previous results (Gouguenheim, 1969; Balkowski, 1973). The internal dispersions of these parameters are comparable to those obtained by Shostak or slightly smaller. They will be analyzed in next sections.

Table 5. M_H/L_0 excess for galaxies and number of their companions

Name (1)	$\Delta[\log(M_H/L_0)]$ (2)	Nc (3)
N 628	0.31 (*)	+5
N 908	−1.10	0
N 925	0.09 (*)	−1
N1042	−0.18 (*)	+5
N1232	0.02	−1
N1337	0.25 (*)	−2
N1784	0.31	+1
N2613	−0.18	+2
N3003	0.35	0
N3027	0.31 (*)	+2
N3044	−0.02	+3
N3079	−0.01 (*)	0
N3254	0.11	−1
N3319	0.22 (*)	0
N3338	0.34	+4
N3423	−0.09 (*)	+2
N3495	−0.13 (*)	+2
N3511	0.21	−1
N3521	−0.07	+5
N3556	−0.05 (*)	+2
N3642	0.01	+4
N3675	−0.03	−1
N3726	0.03 (*)	+3
N3756	−0.26	+3
N3893	−0.02 (*)	+2
N3938	−0.02 (*)	+4
N4254	−0.17	−2
N4303	−0.13 (*)	+2
N4321	−0.38 (*)	+4
N4517	−0.05 (*)	+2
N4559	0.17 (*)	0
N5364	−0.17	0
N5746	−0.41	+2
N5879	−0.05 (*)	−1
N6015	0.15	−2
N7331	0.02 (*)	+4
N7741	0.05 (*)	+3

Column 1: Identification of the galaxy (NGC)
Column 2: Difference between $\log(M_H/L_0)$ and the mean value $\langle\log(M_H/L_0)\rangle_T$ corresponding to the morphological type of the galaxy (Table 3)
Column 3: Number of companions according to Madore (1980). This number of companions is the remainder after substracting a statistically determined background contribution
(*) M_H/L_0 value taken from Shostak (1978)

VI. Analysis of the Dispersion of the H I Mass to Luminosity Ratio

VI. 1. Relationship with the Neighbourhood of the Galaxy

In order to study the influence of the neighbourhood of a galaxy on its overall properties three different tests have been made using the unbiased sample.

First, all the galaxies having a possible companion at a distance closer than about 10′ have been eliminated of the sample. For each type the mean values of the M_H/L_0 ratio together with the dispersion around this mean values are given in Table 4. It appears that isolated galaxies tend to have, on the mean, a larger H I mass-to-luminosity ratio and that the inclusion in the sample of non-isolated galaxies leads to an increase of the dispersion.

Madore (1980) has shown that spiral galaxies with several close low-luminosity companions (Holmberg, 1969) have a higher luminosity class than spirals with few companions. There are 17 galaxies in common in our unbiased sample and in the sample of 156 galaxies studied by Holmberg; their H I mass-to-luminosity ratio M_H/L_0 is compared in Table 5 to the mean value $\langle M_H/L_0\rangle$ expected

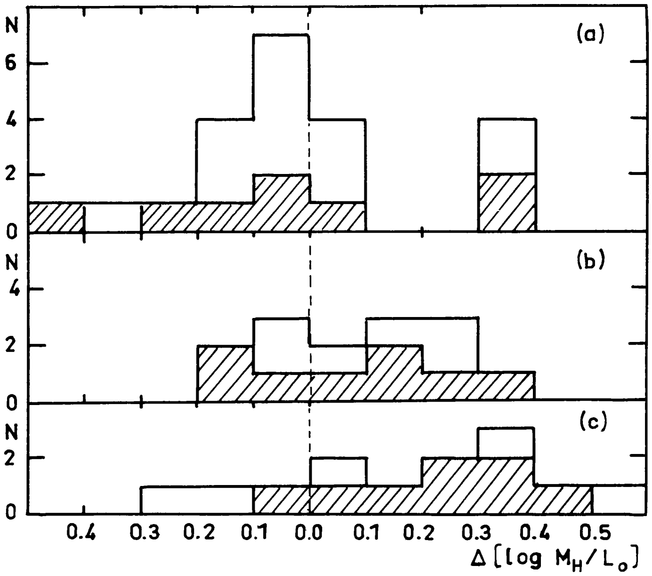

Fig. 10a–c. Histogram of excess M_H/L_0 ratio defined as Δ [log $(M_H/L_0)] = \log (M_H/L_0) - \langle \log (M_H/L_0) \rangle_T$ for galaxies having more than 1 companion according to Madore **a**, for galaxies having 1 or less companion according to Madore **b** (the hatched regions correspond to the present H I data) and for isolated galaxies given by Huchra and Thuan (hatched region) and by Karachentseva and Karachentsev **c**

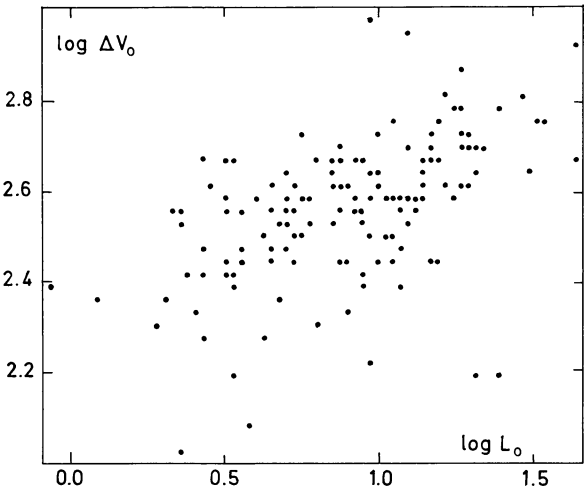

Fig. 11. The line width ΔV_0 (in km s^{-1}), corrected for bandwidth and inclination effects, is plotted against the luminosity (in 10^9 $L_\odot$), both in logarithmic scales, for the unbiased sample of measured galaxies ($2.90 \leq \log V_0 \leq 3.35$)

for their types. For the 10 galaxies having 1 or less close companion, Δ [log (M_H/L_0)] defined as $\log (M_H/L_0) - \langle \log (M_H/L_0) \rangle_T$ is equal on the mean to 0.03 ± 0.09 m.e. For the 7 galaxies having 2 or more companions $\langle \Delta [\log (M_H/L_0)] \rangle = -0.08 \pm 0.09$ m.e. (Fig. 10a, b).

This suggests that isolated galaxies have a larger M_H/L_0 value, but this result is not significantly established. In order to increase the sample we have added all the galaxies studied by Holmberg

Table 6. M_H/L_0 excess for isolated galaxies

Name	Δ [log (M_H/L_0)]	Ref.
N2712	0.17	HT
N3254	0.08	HT
N3319	0.28 (*)	HT
N3930	0.34	HT
N5301	0.30	HT
N5448	−0.01 (**)	HT
N5584	−0.16	K2
N5690	0.04	K2
N5832	0.54 (*)	K2
N5964	0.31	K2
N6012	0.41 (**)	HT
N6015	0.21	HT
N6118	−0.24	K2

Column 1: Identification of the galaxy
Column 2: M_H/L_0 excess defined as in Table 5, Column 2
Column 3: Reference for isolated galaxies: HT (Huchra and Thuan, 1977) K2 (Karachentseva and Karachentsev, 1979)
(*) M_H/L_0 value taken from Shostak (1978)
(**) M_H/L_0 value taken from Bottinelli et al. (1980a)

belonging to the unbiased range and for which Shostak (1978) gives a value of M_H/L_0. This leads to a sample of 37 galaxies. After a 2σ-rejection excluding NGC 628, NGC 908, NGC 3027, and NGC 3368, it comes that for the 15 galaxies having 1 or less companion $\langle \Delta [\log (M_H/L_0)] \rangle = 0.10 \pm 0.05$ m.e. and for the 18 galaxies having 2 companions or more, $\langle \Delta [\log (M_H/L_0)] \rangle = -0.10 \pm 0.03$ m.e. (Fig. 10a and b). This confirms the same trend: isolated galaxies have on the mean a higher H I mass-to-luminosity ratio than galaxies with close companions. This result is consistent with the higher luminosity of galaxies with close companions found by Madore.

A third analysis has been performed using the lists of isolated galaxies by Huchra and Thuan (1977). For the 5 isolated galaxies belonging to our unbiased sample (Table 6) $\langle \Delta [\log (M_H/L_0)] \rangle = 0.22 \pm 0.05$ m.e. (Fig. 10c). The result remains the same when adding two Sa galaxies (Bottinelli et al., 1980a) and one galaxy belonging to Shostak's sample. There are also 5 galaxies of our unbiased sample which are classified as isolated by Karachentseva and Karachentsev (1979). When considering together the 13 above isolated galaxies the excess becomes: $\langle \Delta [\log (M_H/L_0)] \rangle = 0.16 \pm 0.07$ m.e. (Fig. 10c).

Though not very significantly established, the number of points being small, this result indicates the same trend: isolated galaxies appear to have a larger H I mass-to-luminosity ratio. This trend does not necessarily imply that non-isolated galaxies are actually H I deficient. These galaxies could be systematically more luminous as those studied by Madore (1980), the presence of companions being responsible of star formation enhancement.

VI. 2. Does M_H/L_0 Depend on the Luminosity?

It is very difficult to test the variation of $\log M_H/L_0$ against $\log L_0$. The first reason is that M_H/L_0 depends on the morphological type which is correlated to the luminosity: a possible luminosity effect has thus to be disentangled from the type effect. A second and more important problem is the following one. When applying the method of least squares, one assumes that the observable quantities are the sum of an exact variable and a random one, generally assumed to be gaussian, and that the scatters of these observed variables are uncorrelated (this problem is treated by Deeming,

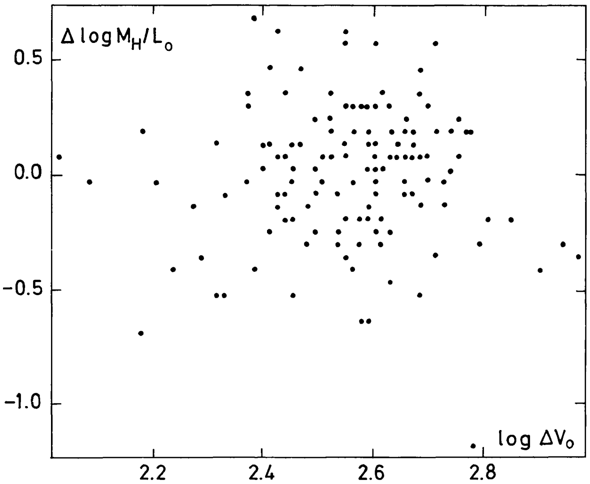

Fig. 12. The M_H/L_0 excess $(M_H/L_0)/\langle M_H/L_0\rangle_T$ is plotted versus the luminosity indicator ΔV_0 (in km s^{-1}) in logarithmic scales. No significant correlation is present

1968). Obviously, this condition is not fulfilled when plotting log M_H/L_0 versus log L_0 because of the scatter in the luminosity.

Thus, to get round both these difficulties, it has been chosen here to plot log (M_H/L_0) versus log (ΔV_0), assuming ΔV_0 to be an indicator of the luminosity, through the Tully-Fisher relation (1977). The scattered gaussian variables attached to M_H/L_0 and ΔV_0 are uncorrelated. Moreover in order to disentangle the type effect from the luminosity effect, log (M_H/L_0) has been plotted against log (ΔV_0) for each class of morphological type.

In order to verify first that ΔV_0 is correlated to the luminosity, log (ΔV_0) has been plotted against log L_0 for each class of morphological type and for the restricted range of velocity defined avove. The correlation is significant at the 0.01 probability level for types 3–6. The correlation is not significant for the last class of types ($T \geqq 7$), but the general trend can be recognized. The population is small ($n=18$) and the lack of correlation could be due to one aberrant point. The log (ΔV_0) – log L_0 relation is shown in Fig. 11 for all the galaxies of our restricted sample (all types being mixed); it remains the same if the whole velocity range is considered. This correlation is extensively discussed in another paper (Bottinelli et al., 1980c).

As a second step, we have looked for a possible correlation between log (M_H/L_0) and log (ΔV_0) for each type T, for our unbiased sample. The result is negative: none of the correlation is significant, even at the 0.05 probability level of error. No more significant correlation appears when mixing all the types together as shown in Fig. 12, where log $[(M_H/L_0)/\langle M_H/L_0\rangle_T]$ is plotted versus log (ΔV_0). This result confirms that found by Shostak (1978) and Bottinelli et al. (1980a): the hydrogen content does not vary systematically with luminosity within a morphological type. However a contradictory result is expected as noted by Strom (1980) in the model of galactic shock-driven star formation in spiral arms, when considering the disc luminosity instead of the total luminosity; as within a type, the disc luminosity is expected to be a constant fraction of the total luminosity, our H I results to not give support to this model. However it can be noted that Δ [log (M_H/L_0)] seems to be smaller for log (ΔV_0) larger than 2.8 (Fig. 12). If real this effect can be compared to the one obtained by Sullivan et al. (1981) who suggested that within a given Hubble type, M_H/L_0 falls once L_0 crosses a threshold level.

VII. Conclusion

The present study of the H I integral properties of a large number of spiral galaxies has brought to light the following points:

1. Our unbiased sample of galaxies with type going from Sa to late-spiral shows a continuous, well-defined variation of H I parameters.
2. The internal dispersions of distance dependent parameters, within a given type, are reduced when accurate distances determined by de Vaucouleurs are used, instead of assuming a constant Hubble flow.
3. Part of this scatter is intrinsic and related to the relation of the galaxies with their neighbourhood: the scatter is reduced when eliminating galaxies with nearby companions.
4. Isolated galaxies seem to have a larger H I mass-to-luminosity ratio.
5. The decrease of M_H/L_0 with increasing luminosity previously found and expected from theoretical reasons, is not confirmed when using unbiased samples and the corrected line-widths as an indicator of the luminosity, through the Tully-Fisher relation.

Acknowledgements. We thank Mme Nicole Hallet for help in the obervations, Mme Nicole Durand for help in the data reduction and Pr. de Vaucouleurs for kindly communicating unpublished and updated determinations of distance moduli.

Appendix. Transformation of Zwicky Magnitudes into B_T Magnitudes

The original magnitudes m_{Zw} given in the CGCG (Zwicky et al., 1961–1968) are first corrected for two perturbing effects (surface brightness effect and "volume-number" effect) to transform them into magnitudes m_H in the Holmberg (1958) photographic system, according to the relation given by Paturel (1979, Eq. (13)):

$$m_H = 0.89\ m_{Zw} - 0.28 \log (100\ a_{25} b_{25}) + C_i, \qquad (1)$$

where a_{25} and b_{25} are observed major and minor axes in arc min, and C_i a constant depending on the volume number (I–VI) of the CGCG.

Then the Holmberg magnitudes are reduced to the B_T system using the relation given in the RC2:

$$B_T = m_H + 0.19 - 0.13\ c, \qquad (2)$$

where c is the colour index.

Taking into account relations (1) and (2), the reduced magnitudes B_T^{Zw} are obtained from the relation:

$$B_T^{Zw} = 0.89\ m_{Zw} - 0.56 \log (10\ a_{25}) + 0.28 \log R_{25} + C_i + 0.19 - 0.13\ c, \qquad (3)$$

where $R_{25} = a_{25}/b_{25}$.

The colour index c has been evaluated from the morphological type T using the following $c - T$ relationship established from the original Holmberg catalogue (1958):

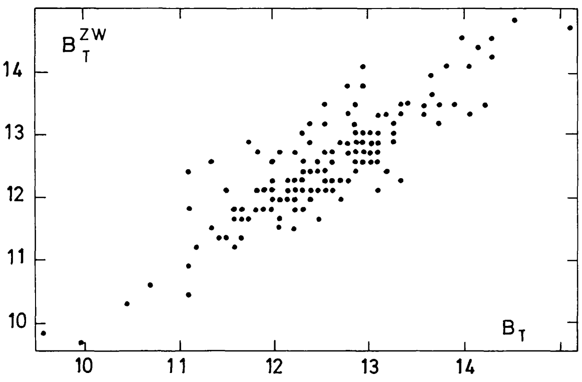

Fig. 13. Comparison between B_T magnitudes given in the RC2 and B_T^{Zw} magnitudes determined from Zwicky's magnitudes reduced to the B_T system

Type T	c
2	0.707
3	0.731
4	0.564
5	0.489
6	0.444
7	0.401
8	0.399
9	0.306
10	0.314

In the previous paper (Bottinelli et al., 1980a) the same procedure was used, but the sample was too small to allow a significant comparison (moreover, only few galaxies were treated by this procedure). Figure 1A shows the relation between B_T^{Zw} and B_T for all galaxies in our sample for which both quantities are available. The linear regression described as $B_T^{Zw}=sB_T+\text{cst.}$ corresponds to $s=1.05\pm0.04$ ($\varrho=0.90$ and $n=161$), 4 points being excluded from a 3σ-rejection. The slope s is not significantly different from one, which means that there is no deviation from linearity in the scale of our reduced system. When adopting a slope 1, the difference $\langle(B_T^{Zw}-B_T)\rangle$ is equal to -0.021 ± 0.030, which means that there is no zero point difference. However it should be noted that the reduction formula (3) is established only up to $m_{Zw}=14.5$.

References

Balkowski, C.: 1973, *Astron. Astrophys.* **29**, 43
Balkowski, C., Chamaraux, P.: 1981, *Astron. Astrophys.* **97**, 223
Bottinelli, L.: 1971, *Astron. Astrophys.* **10**, 437
Bottinelli, L., Gouguenheim, L.: 1974, *Astron. Astrophys.* **36**, 461
Bottinelli, L., Gouguenheim, L., Paturel, G.: 1980a, *Astron. Astrophys.* **88**, 32
Bottinelli, L., Gouguenheim, L., Paturel, G.: 1980b, *Astron. Astrophys. Suppl. Ser.* **40**, 355
Bottinelli, L., Gouguenheim, L., Paturel, G., de Vaucouleurs, G.: 1980c, *Astrophys. J.* **242**, L153
Bottinelli, L., Gouguenheim, L., Paturel, G.: 1981, *Astron. Astrophys. Suppl. Ser.* **44**, 217
Bottinelli, L., Gouguenheim, L., Paturel, G.: 1982a, *Astron. Astrophys. Suppl. Ser.* **47**, 171
Bottinelli, L., Gouguenheim, L., Paturel, G.: 1982b, *Astrophys. Suppl. Ser.* (submitted)
Chamaraux, P., Balkowski, C., Gerard, E.: 1980, *Astron. Astrophys.* **83**, 38
Deeming, T.J.: 1968, Vistas in Astronomy, ed. A. Beer, Vol. **10**, 125
Gallouët, L., Heidmann, N.: 1971, *Astron. Astrophys. Suppl. Ser.* **3**, 325
Gallouët, L., Heidmann, N., Dampierre, F.: 1973, *Astron. Astrophys. Suppl. Ser.* **12**, 89
Gallouët, L., Heidmann, N., Dampierre, F.: 1975, *Astron. Astrophys. Suppl. Ser.* **19**, 1
Gouguenheim, L.: 1969, *Astron. Astrophys.* **3**, 281
Heidmann, J., Heidmann, N., de Vaucouleurs, G.: 1972, *Mem. Roy. Astron. Soc.* **75**, 85, 105, and 121
Holmberg, E.: 1958, *Medd. Lunds Obs. Ser.* II, 136
Holmberg, E.: 1969, *Arkiv. Astron.* **5**, 305
Huchra, J.P., Thuan, T.X.: 1977, *Astrophys. J.* **216**, 694
Huchtmeier, W.K., Tammann, G.A., Wendker, H.J.: 1976, *Astron. Astrophys.* **46**, 381
Karachentseva, V.E., Karachentsev, I.D.: 1979, *Astrofisika* **15**, 589
Krumm, N., Salpeter, E.E.: 1979, *Astrophys. J.* **227**, 776
Lewis, B.M., Davies, R.D.: 1973, *Monthly Notices Roy. Astron. Soc.* **165**, 213
Madore, B.F.: 1980, *Astron. J.* **85**, 507
Malmquist, K.G.: 1920, *Medd. Lunds Obs. Ser.* 2, No. 22
Nilson, P.: 1973, Uppsala General Catalogue of Galaxies (UGC), Uppsala Astr. Obs. Ann. 6
Paturel, G.: 1979, *Astron. Astrophys.* **71**, 19
Roberts, M.S.: 1969, *Astron. J.* **74**, 859
Roberts, M.S.: 1976, in *Stars and Stellar System*, Vol. IX, Univ. of Chicago Press, Chicago
Roberts, M.S.: 1978, *Astron. J.* **83**, 1026
Shostak, G.S.: 1978, *Astron. Astrophys.* **68**, 321
Strom, S.E.: 1980, *Astrophys. J.* **237**, 686
Sullivan, W.T.III, Johnson, P.E.: 1978, *Astron. J.* **225**, 751
Sullivan, W.T.III, Bothun, G.D., Bates, B.: 1981, *Astron. J.* **86**, 919
Tully, R.B., Fisher, J.R.: 1977, *Astron. Astrophys.* **54**, 661
de Vaucouleurs, G., de Vaucouleurs, A., Corwin, H.G.: 1976, Second Reference Catalogue of Bright Galaxies, University of Texas Press, Austin
de Vaucouleurs, G.: 1979, *Astrophys. J.* **227**, 729
de Vaucouleurs, G., Bollinger, G.: 1979, *Astrophys. J.* **233**, 433
Zwicky, F., Herzog, E., Wild, P., Karpowicz, M., Kowal, C.T.: 1961, 1968, Catalogue of Galaxies and Clusters of Galaxies, I–VI (CGCG), California Institute of Technology, Pasadena